POLITECNICO
MILANO 1863

SCUOLA DI INGEGNERIA INDUSTRIALE
E DELL'INFORMAZIONE

Exploring the solid-state synthesis and host-guest chemistry of M12L8 poly-[n]-catenanes using the tris-pyridyl benzene ligand

Tesi di laurea magistrale in

CHEMICAL ENGINEERING
INGEGNERIA CHIMICA

Author: **Stefano Elli**

Student ID: **953188**
Advisor: **Prof. Javier Martí-Rujas**
Co-advisor: **Dott. Manfredi Caruso**
Academic Year 2021-22

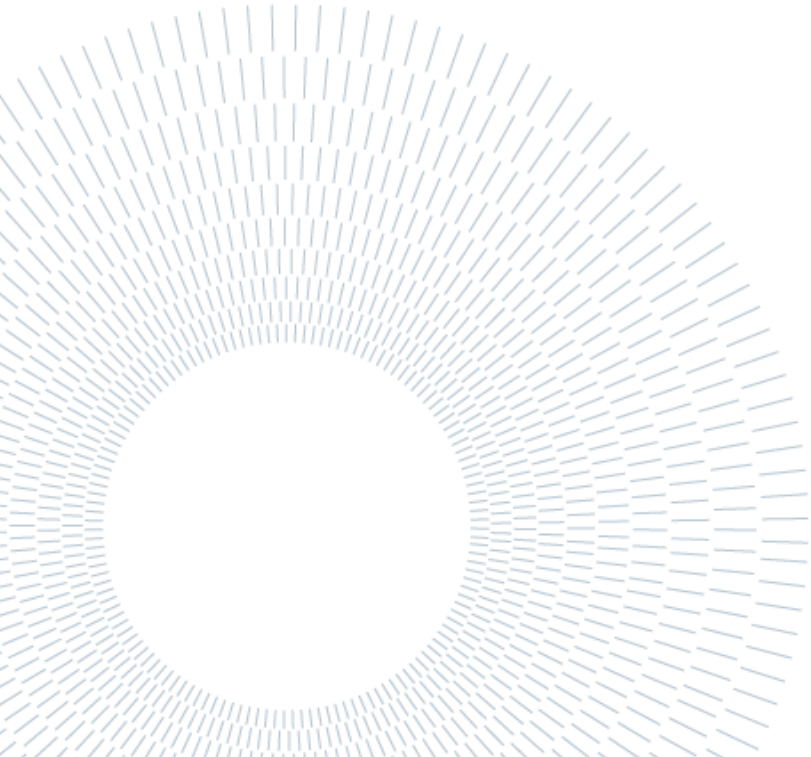

Abstract

Studies on polycatenanes began in the mid-1950s and have always intrigued experts because of their interesting structure and difficulty in synthesis. Polycatenanes are classified as Mechanically Interlocked Molecules (MIMs), as they are formed by the interlocking of multiple molecular fragments which, through mechano-chemical bonds, give topologies reminiscent of a chain. For metal-organic MIMs, the molecular fragments are formed by coordination bonds between organic ligands and secondary units, i.e. metal salts. Their architecture, which is related to that of metal-organic frameworks (MOFs), as are formed by the self-assembly of metal ions and organic ligands, opens up a world of possibilities when it comes to their application in a wide range of research fields.

Following the recent article on $M_{12}L_8$ polycatenane $[(ZnX_2)_{12}(TPB)_8]$ (where M is Zn(II) and L is the ligand tris-pyridyl benzene (TPB)), we wanted to continue and explore the subject further, both in terms of synthesis and applications. From a sustainable perspective, the aim of the project was toward a solvent-free synthesis. In this way, we were able to synthesize the same $[(ZnX_2)_{12}(TPB)_8]$ poly-[*n*]-catenane upon grinding TPB with zinc salts. Various experimental techniques such as X-ray crystallography, IR, thermogravimetrical, and elemental analysis were used to characterize the products obtained in the solid-state reactions. Powder XRD demonstrated that the products were amorphous. Crucially, the amorphous phase can undergo a transformation to crystalline upon immersion in aromatic solvents which exert a templating effect. In order to investigate the potential applications of this material, we focused on molecular storage and the separation of isomers. For the separation of isomers, the three isomers of dichlorobenzenes were chosen. The second part of this project was focused on the synthesis of new exo-tridentate ligands to replace TPB in the polycatenane structure. We were able to isolate and characterize functionalized TPBs to which chlorine and methyl groups were attached. Finally, in support of a green approach, we have shown that it is possible to recover pure TPB by simply immersing polycatenane in water, allowing for the reuse of the organic ligand.

Key-words: poly-[*n*]-catenane; mechanochemistry; molecular storage; isomer recognition; ligand diversification.

Abstract in italiano

Gli studi sui policatenani sono iniziati a metà degli anni '50 e hanno sempre incuriosito gli esperti per la loro interessante struttura e difficoltà sintetica. I policatenani sono classificati come Mechanically Interlocked Molecules (MIMs), in quanto sono formati dalla concatenazione di più frammenti molecolari che, attraverso legami meccano-chimici, generano topologie che richiamano quella di una catena. I composti MIM metallo-organici, sono costituiti da frammenti molecolari formati da legami di coordinazione tra un ligando organico e un'unità secondaria, cioè un sale metallico. La loro architettura, che è legata a quella dei MOF in quanto formati anch'essi dall'auto-assemblaggio di ioni metallici e ligandi organici, apre un mondo di possibilità riguardo la loro applicazione in una vasta gamma di campi di ricerca.

Dopo il recente articolo sul policatenano $M_{12}L_8$ $[(ZnX_2)_{12}(TPB)_8]$ (dove M è Zn(II) e L è il ligando tris-piridil benzene (TPB)), abbiamo voluto esplorare ulteriormente l'argomento, sia in termini di sintesi che di applicazioni. In una prospettiva di chimica sostenibile, l'obiettivo del progetto è stato diretto verso una sintesi senza solventi. In questo modo, siamo stati in grado di sintetizzare lo stesso $[(ZnX_2)_{12}(TPB)_8]$ poli-[*n*]-catenano per semplice grinding del TPB con i sali di zinco. Varie tecniche sperimentali come la cristallografia a raggi X, l'IR, la termogravimetria e l'analisi elementare sono state utilizzate per caratterizzare i prodotti ottenuti nelle reazioni allo stato solido. Le analisi di PXRD hanno dimostrato che i prodotti erano amorfi. In particolare, la fase amorfa può subire una trasformazione in cristallina dopo l'immersione in solventi aromatici per effetto templante. Al fine di indagare le potenziali applicazioni di questo materiale, ci siamo concentrati sull'immagazzinamento molecolare e sulla separazione degli isomeri. Per la separazione degli isomeri, sono stati scelti i tre isomeri strutturali del diclorobenzene. La seconda parte di questo progetto è concentrata sulla sintesi di nuovi ligandi eso-tridentati per sostituire il TPB nella struttura del policatenano. Siamo stati in grado di isolare e caratterizzare diverse forme di TPB funzionalizzato a cui sono stati attaccati gruppi cloro e metile. Infine, a sostegno di un approccio "green", abbiamo dimostrato che è possibile recuperare il ligando TPB praticamente puro per semplice immersione in acqua, in modo da poter poi essere riutilizzato.

Parole chiave: poly-[*n*]-catenane; meccanochimica; immagazzinamento molecolare; riconoscimento isomeri; diversificazione ligandi.

Contents

Abstract ... **iii**

Abstract in italiano ... **v**

Contents ... **vii**

1 Introduction ... **1**

1.1 Metal-Organic Frameworks ... 1

1.1.1 Definition and historical background ... 1

1.1.2 Applications ... 4

1.2 Catenanes ... 11

1.3 $[(ZnX_2)_{12}(TPB)_8]$ Poly-[*n*]-catenane: a case of study ... 15

1.4 Toward green chemistry ... 17

1.5 Ligand diversification ... 19

2 Results and discussions ... **21**

2.1 Mechanochemical synthesis ... 21

2.2 Applications ... 29

2.2.1 Molecular storage ... 29

2.2.2 Isomer recognition ... 35

2.3 Diversification ... 39

3 Materials and methods ... **45**

3.1 Analytical Instrumentation ... 45

3.2 General Procedures ... 46

3.2.1 Catenanes Synthesis ... 46

3.2.2 Adsorption Experiments ... 47

3.2.3 Isomers Separation Experiments ... 48

3.2.4 Ligand Synthesis 48

4 Conclusions and further studies 55

Bibliography 57

List of Figures 68

***Ringraziamenti* 73**

1 Introduction

1.1 Metal-Organic Frameworks

1.1.1 Definition and historical background

To clarify the field of solid-state coordination chemistry that is addressed in this thesis, it is useful to start with some concise definitions. First of all, those of Coordination Polymer (CP), Coordination Network (CN), Metal-Organic Frameworks (MOFs). According to IUPAC, Coordination Polymers are defined as: *"A coordination compound with repeating coordination entities extending in 1, 2, or 3 dimensions"*. [1] Examples of coordination polymers are the Hofmann compounds with the formula $Ni(CN)_2(NH_3)(C_6H_6)$, typically used for the separation of hydrocarbons, especially xylenes. Coordination Networks are instead described as *"A coordination compound extending, through repeating coordination entities, in 1 dimension, but with cross-links between two or more individual chains, loops, or spiro-links, or a coordination compound extending through repeating coordination entities in 2 or 3 dimensions"*. [1] Starting from the two previous definitions, we arrive at the description of the meaning of MOF defined by IUPAC as: *"a coordination network with organic ligands containing potential voids"*. [1] Thereby, it can be deduced that MOFs are compounds with dynamic behavior and characterized by an intrinsic high porosity that ensures their use in a wide range of transversal applications (Figure 1.1). [2, 3, 4]

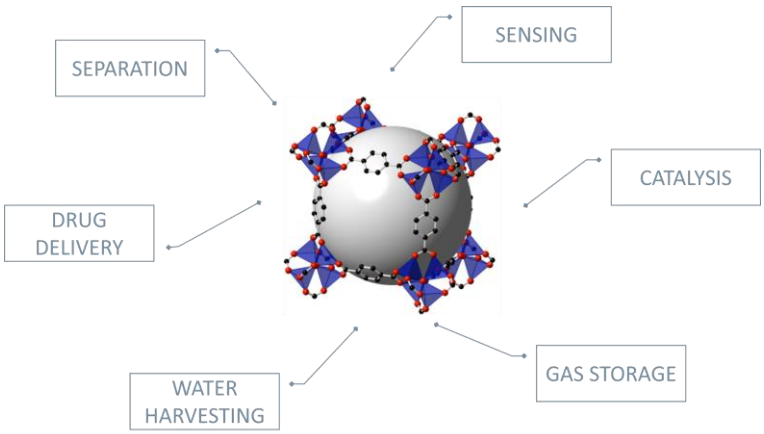

Figure 1.1: MOF applications[86]

MOFs can be depicted as structures built on organic ligands and inorganic Secondary Building Units (SBUs) that assemble with a specific topology and show predictable structural properties. Inorganic SBUs are metal ions or clusters able to strongly bound linear or branched organic ligands. The result is a net showing voids that can act as hosts for a wide range of guests (*e.g.* molecules, complexes, proteins). [5, 6, 7] The possibility to tune the dimension and the size of these voids started a challenge between research groups working in this context for the synthesis of the MOF with the largest internal surface area. The current record is represented by NU-109 and NU-110, synthesized by Hupp and co-workers. [8] Apart from this scientific challenge, the synthesis of MOFs with extremely high internal surface area is particularly attractive for their use at an industrial level as storage materials for gases (*e.g.* hydrogen, methane, carbon dioxide). [9]

The inception of MOFs derives directly from zeolites whose field of research began in the 1940s. Zeolites are crystalline aluminosilicates that express high surface area and pores with dimensions up to 2 nm. [10] As expected, they have a great role in the industrial field but there is not a boundless variety of zeolites considering both natural and synthetic ones. To tackle this problem, studies in the coordination chemistry field to find a competitor started back in 1964 [11] but it was only in the '90s, with the publications of Hoskins and Robson, [12, 13] that the first porous coordination polymers were disclosed. A few years later, in 1995, "Metal-Organic Frameworks" began their rise thanks to studies conducted by Omar Yaghi *et al.* [14, 15] From that point on, many published structures have been categorized and renamed according to a specific nomenclature. MOFs having the same topology

have equal prefixes, such as those with the same symmetry (Isoreticular Metal-Organic Frameworks, *e.g.* IRMOF1-IRMOF16) or those with zeolite topology (Zeolite Imidazolate Framework, *e.g.* ZIF-8). Some MOFs are named with the abbreviation of the university or the research center where they were discovered (*e.g.* UiO, MIL, HKUST).

The main advantage of MOFs over zeolites lies in the great interchangeability between the organic ligands and the inorganic SBUs, which gives rise to a vast number of possible structures. [5] Moreover, differently from zeolites, MOFs' ligands can be easily modified even after synthesis through a process known as post-synthetic modification. [16] As a result, starting from a MOF it is possible to synthesize a series of differently functionalized isoreticular structures with retained topology but tunable properties.

In recent years, this great operational freedom allows for the development of several operating conditions and synthetic routes which, starting from the same initial reagents, generate different structures. Therefore, the number of MOF structures identified and reported in the Cambridge Structural Database is more than 100,000 and continues to grow (Figure 1.2). [4]

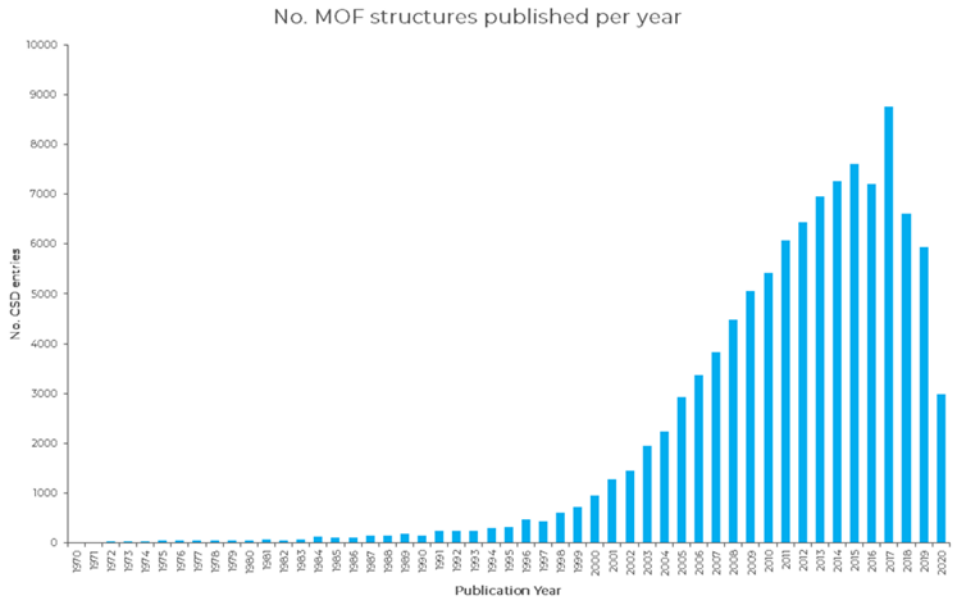

Figure 1.2: MOF publications per year[88]

Simultaneously, the potential applications of MOFs at an industrial level have pushed toward the development of scaled processes for their synthesis. To this end, in recent years several dedicated companies and start-ups have been established (*e.g.* Framergy, MOF Technologies, EnergyX, MOF4Air), confirming the high interest in the field.

1.1.2 Applications

It is now useful to briefly discuss some of the most notable applications of MOFs demonstrating the importance of these materials.

As mentioned in the previous section, the potential applications of MOFs are almost unlimited. [17, 18, 19] Just to give a few examples, MOFs have demonstrated peculiar properties in a variety of different fields such as catalysis, [20, 21, 22] biomedicine, [23, 24] and sensing [25] applications up to their use as nanoreactors or molecular flasks. [26] Given the broadness of this research field, only a few of the most promising and remarkable applications are illustrated below.

1.1.2.1 Gas Storage

As already discussed, the permanent porosity and the high internal surface areas of MOFs suggested the possibility of their use for storage purposes. Indeed, one of the first and most targeted applications of MOFs is gas storage, with particular attention to hydrogen and methane.

Hydrogen storage

Nowadays hydrogen is considered a concrete possibility to definitively replace the use of fossil fuels for energy production in view of the so-called 'Energy Transition'. [27, 9] Over the past few decades, many efforts have been and still are made for the development of efficient hydrogen-based fuel cells. The ultimate goal is to create a closed production cycle where energy and water are the only "by-products" and hydrogen is regenerated by photoelectrolysis, thus implementing the so-called 'Hydrogen Economy'. [28] One of the major unsolved problems limiting the definitive implementation of these processes is, in fact, the storage of gaseous hydrogen. Currently, the most diffused methods for hydrogen storage are in cryogenic tanks as a liquid or in pressurized tanks as a gas. However, as it is easy

to imagine, both these solutions are impractical and expensive since the former requires energy for the conversion of gaseous hydrogen to a liquid, while the latter requires bulky tanks to retain high pressures. Therefore, an alternative methodology must be found. A potential solution could be the use of adsorbent materials able to reversibly bind hydrogen molecules through weak interactions (*e.g.* Van der Waals interactions). MOFs have emerged as ideal candidates to this end showing outstanding properties. Hydrogen storage in MOFs has been achieved both at low and at room temperature. Reasonably, cryogenic temperature storage provides higher uptake of hydrogen compared to that at room temperature, with the obvious drawback of the energy-consuming thermal conditions. Under these conditions (typically 77 K, 100 bar), an hydrogen uptake of around 9 wt% is usually observed. [27] As previously mentioned, in MOFs the absorption of gaseous hydrogen is a chemisorption process in which hydrogen molecules are directly bound to MOFs through Van der Waals interactions. [9] Thus, MOFs having large voids are undesirable for this purpose as H_2 molecules in the central part of the pores do not take part in these interactions. Making interpenetrated MOFs is an attractive alternative to reduce pore size. At room temperature, hydrogen uptake is lower than 1 wt%. [27] This is mainly due to the weakening of Van der Waals interactions caused by the greater mobility of guest gaseous molecules. A possibility to overcome this limitation proved to be the design of specific MOFs bearing sites with high positive charge density which can strongly polarize H_2 molecules to strengthen the host-guest interaction and increase the storage capacity. [28]

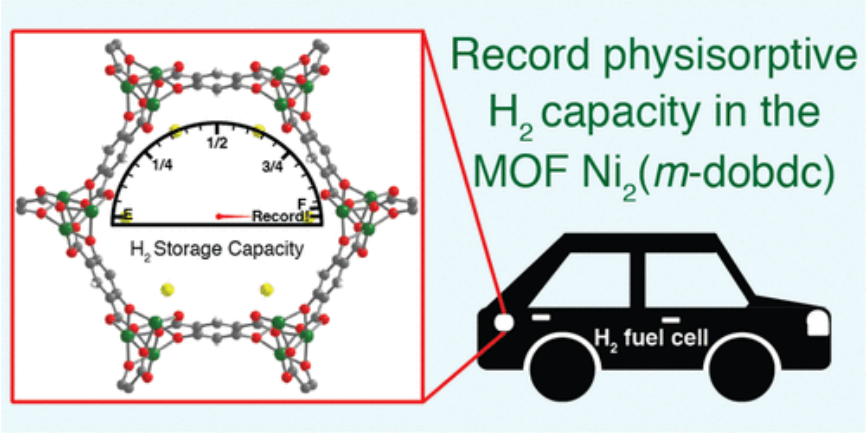

Figure 1.3: MOF for hydrogen storage in fuel cells[28]

Particularly, one practical example with optimal results was reported by Long *et al.* (Figure 1.3), [28] who studied a case of hydrogen storage for near ambient temperature conditions (and pressure in the range 5-100 bar). The MOFs involved are Co_2(*m*-dobdc) and Ni_2(*m*-dobdc) which belong to the family of MOF-74. [29] Synthesized by the coordination between 2,5-dioxido-1,4-benzenedicarboxylate ligand with two different molecules of pyramidal metal(II) salts in a DMF environment, the formed structure is a honeycomb framework that shows different properties and guest affinities depending on the chosen metal.

As shown in Figure 1.4, in the MOF-74 family the fraction of void is very high, with reported pore volumes of 0.53 cm^3/g for the cobalt MOF and 0.56 cm^3/g for the nickel one. Both materials were tested for H_2 adsorption experiments at several temperatures in the range of -75 – 100 °C (-40 °C is the typical storage temperature in fuelling stations). [30] The different isotherms are shown in Figure 1.5.

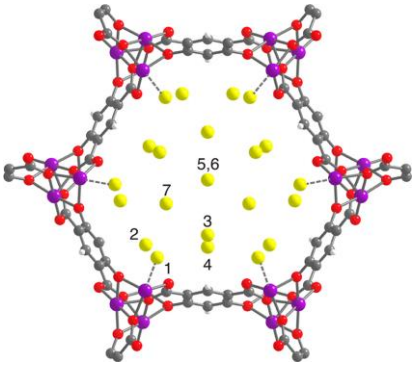

Figure 1.4: Co_2(*m*-dobdc) pore[28]

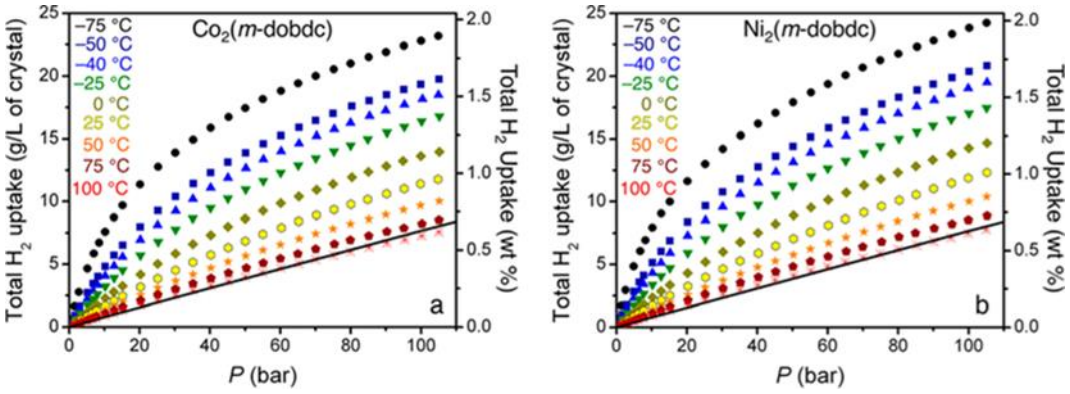

Figure 1.5: H_2 adsorption isotherm of Co_2(*m*-dobdc) and Ni_2(*m*-dobdc) MOFs [28]

The nickel MOF is the most promising one at every temperature and pressure, reaching a peak of 23.8 g of H_2 over L of crystal. At room temperature and a pressure of 100 bar, the amount of hydrogen is 11.9 g/L, and considering that at the release pressure of 5 bar, 0.9 g/L are still retained in the material, the total usable capacity is 11 g/L, which is a reasonable value with respect to compressed hydrogen storage. This important storage capacity is due to a high fraction of Ni^{2+} adsorption sites, which can take part in stronger bonds with respect to Co^{2+}.

Methane storage

Methane, [9, 31] which is the main component of natural gas, is another alternative to liquid hydrocarbon fuels, but the problem is its low volumetric energy density in normal conditions. Increasing this value means, as for hydrogen, compressing it (Compressed Natural Gas) or liquefying it (Liquefied Natural Gas), falling again into the same practical problems. Also in this case, the solution can be the same: the use of adsorbing materials (Adsorbed Natural Gas) with high uptake capacity and delivery ability under reduced pressure. These properties are strictly linked to the type of interactions and the framework (*i.e.* host-guest interactions). It was found that also the dynamic behavior of the framework can enhance the deliverable amount of methane. Having a flexible structure allows that at high pressure with the opening of the cages more gas can be stored, while reducing the pressure the cages will decrease their dimensions allowing just a small quantity to remain in them.

1.1.2.2 Water Harvesting

Water demand is certainly a huge problem that is beginning to affect the world due to climate change and population growth. Numerous research groups worldwide are looking for solutions to this problem. One of them could be the extraction of water from the air. However, the direct condensation of water from the atmosphere requires a great deal of energy, especially in areas with low relative humidity. Prof. Yaghi's group found a possible solution by using MOFs for the collection of pure water even in desert territories. [32, 33] The superior performance of MOFs over other porous structures relies on the higher chemical and thermal stability of these materials over time. Water collection in MOFs occurs both chemically, through the formation of hydrogen bonds between the water molecules and the framework, and physically, through inclusion and capillarity forces. This study is based on the diurnal thermal excursions associated with cycles of water adsorption and desorption in the MOF (Figure 1.6).

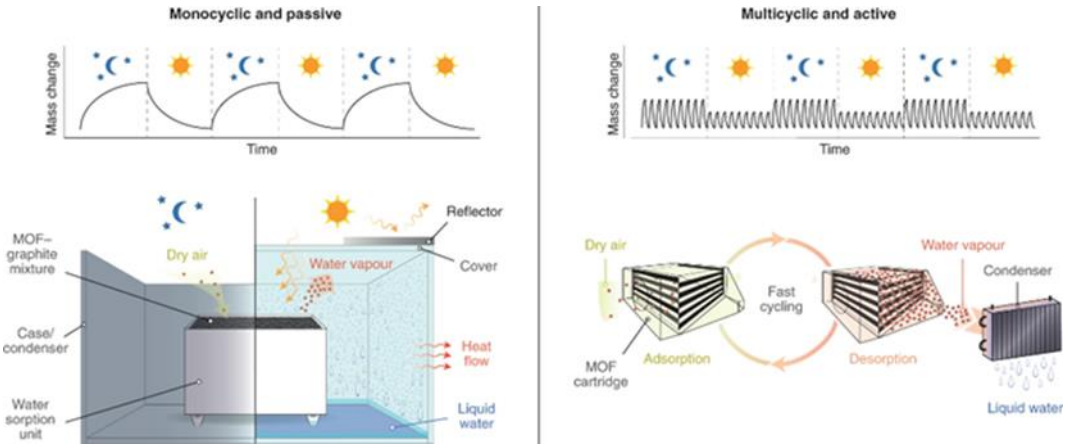

Figure 1.6: MOF water harvesting devices using MOFs [33]

The water collection device can be constructed to perform a single adsorption/ desorption cycle per day or several cycles within the same day when higher productivity is required. 'Monocyclic' devices, exploiting the diurnal thermal excursion, collect water during the night when relative humidity is highest and releases it during the day under solar heat radiation. On the other hand, 'multicyclic' devices guarantee continuous production of water with higher productivity during the night and lower productivity during the day. The only drawback of the multicyclic device is that a condenser is required to operate during the night when there is no solar radiation. It is noteworthy that only pure water is obtained during the process and no waste material is produced. Moreover, the study revealed that the most common water contaminants are not bound as strongly as water molecules, thus avoiding the clogging of the pores and ensuring a longer duration of use of the material.

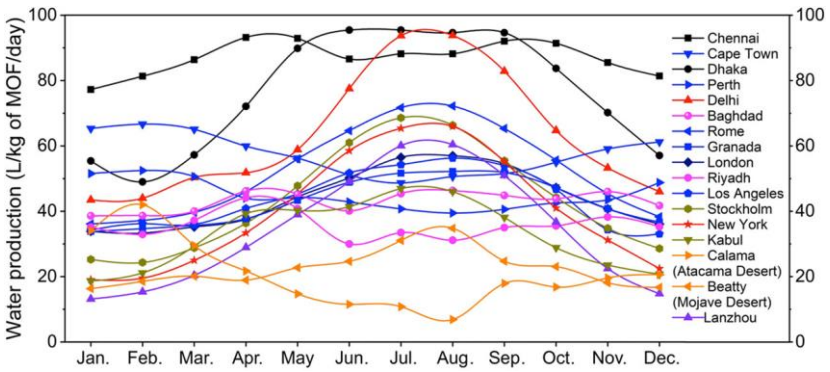

Figure 1.7: Water production in a year for several locations [32]

The results have proved very promising. As can be seen from Figure 1.7, different amounts of water can accumulate depending on location and climate. For example, in the humid conditions of countries such as India or Bangladesh in summer, up to 90 liters of storage per kg of MOF per day can be achieved. In arid areas, such as the deserts of Chile or California studied here, considerable quantities can be obtained, which can exceed 7 liters even in summer seasons when extreme drought conditions are reached.

1.1.2.3 Molecular separation

The study of molecular separation is fundamental in every field of chemistry, ranging from petroleum refining to the pharmaceutical industry. [34] To this end, one of the most used techniques is chromatographic separation. [35] This is a physical separation method in which a mixture of analytes is forced, by means of a carrier (mobile phase), through a column or a capillary packed with a liquid or a solid (stationary phase). The separation of the different analytes is based on the different strengths of the interactions (*i.e.* mainly electrostatic) they establish with the mobile and stationary phases. As a result, analytes are retained with more or less effectiveness, coming out from the column or capillary at different times. Concerning the mobile phase either gases, as in gas chromatography (GC), or liquids, in liquid and high-performance liquid chromatographies (LC and HPLC, respectively), can be used. As for the stationary phase, a porous solid material is typically used (*e.g.* silica, alumina). Thanks to their properties, MOFs could represent a useful tool also in the field of separation chromatography. With the possibility of engineering their pore size and shape and introducing functional groups into the structure to target specific interactions, MOFs are ideal candidates for their use as stationary phases. Indeed, several reported examples exist of their use in GC, LC, and HPLC chromatographies. [36] Compared to the already existing stationary phases, MOFs possess particularly attractive advantages. As an example, their permanent high porosity allows keeping a high flow of the mobile phase even at low pressures. Moreover, the possibility to easily functionalize MOFs' organic ligands allows for the creation of specific recognition sites able to separate not only different molecules but even stereoisomers (Figure 1.8). [37]

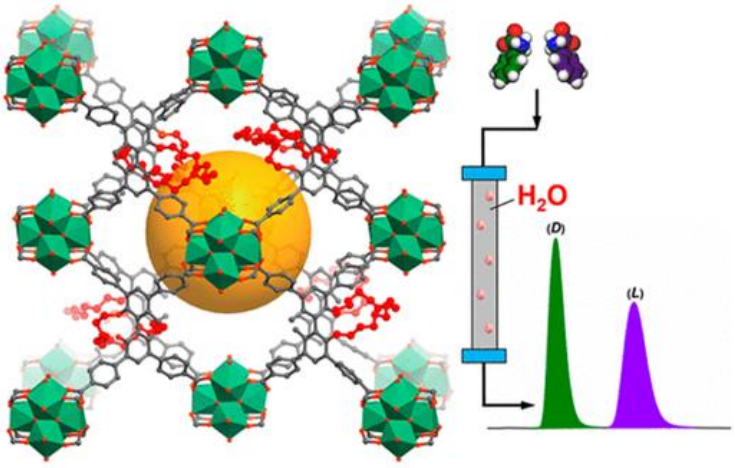

Figure 1.8: MOFs applied to chromatographic columns[37]

In this regard, chromatography is particularly useful when applied in the pharmaceutical industry. Most drugs derive from the isolation of a single enantiomer of a molecule. Given the dimensions of usual drug-related molecules, when MOFs are designed to be chiral stationary phases, the ligand must be large to generate big enough pores. To provide an example, a triazole-based metal-organic framework (TAMOF-1) was appropriately designed for the enantioselective separation of molecules in liquid chromatography. [38] Particularly, in the case of separation of a racemic solution of (±)-ibuprofen, a common anti-inflammatory drug, where the (*S*)-enantiomer is much more active with respect to the (*R*) one. TAMOF-1 is a crystalline MOF synthesized at room temperature by linking a histidine-derived ligand and a copper salt in a water solvent ($[Cu(S\text{-}TA)_2]\cdot_n H_2O$) (Figure 1.9). The generated MOF is filled with water molecules but keeps the framework upon dehydration, showing a solvent-accessible volume of 3307 $Å^3$. A column was then packed with the material and the racemic solution, diluted in acetonitrile, was passed through. As shown by the chart, *S*-ibuprofen has a lower retention time, meaning it has fewer interactions with the stationary phase with respect to the (*R*)-enantiomer (Figure 1.10). With this process, the two products are recovered with high yields at room temperature and near-atmospheric pressure.

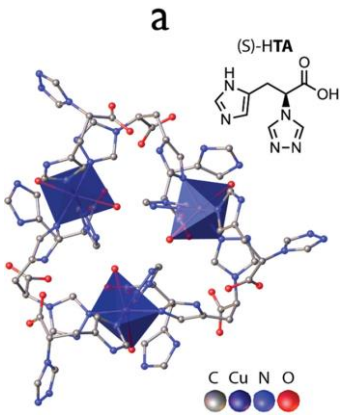

Figure 1.9: TAMOF-1 crystal structure[38]

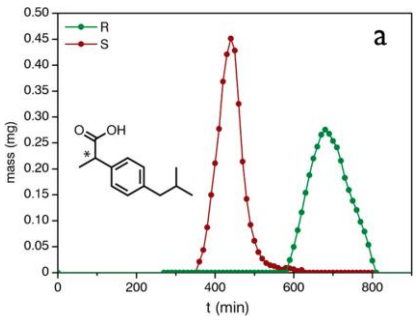

Figure 1.10: Liquid Chromatography of (±)-ibuprofen[38]

1.2 Catenanes

To be precise, the compounds I have been synthesizing over the past few months and which I am discussing here belong to a category of supramolecular chemistry that rather than MOFs are MIMs (Mechanically Interlocked Macromolecules). Precisely defined as Catenanes, are defined by IUPAC as: *"Hydrocarbons having two or more rings connected in the manner of links of a chain, without a covalent bond. More generally, the class catena compounds embraces functional derivatives and hetero analogues"*. [39] Interpenetrating one macrocycle to another, we obtain a chain-like oligomer or polymer that can be broken up only by breaking one macrocycle. If the number of macrocycles in the same chain is large, we obtain a poly-[*n*]-catenane, where n is the number of macrocyclic units, with a similar relationship to that between monomers and polymers but from which they differ in topology and properties. The latter called polycatenanes are the object of study for over 70 years, [40] and were first proposed, without being synthetized, by Frisch et al. in 1953 [41] and by Patat and Derst in 1959. [42]

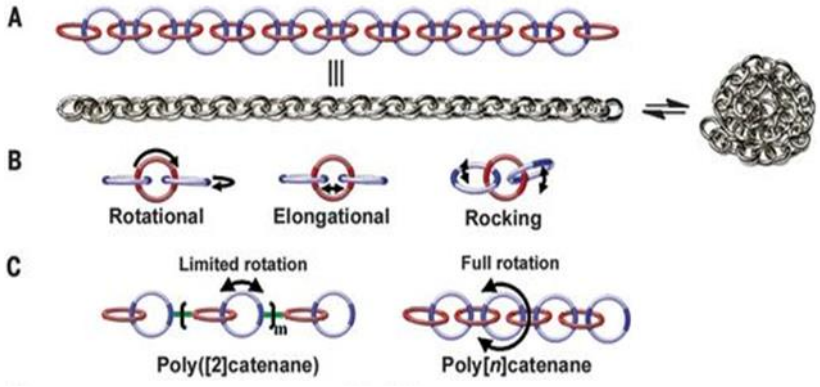

Figure 1.11: Polycatenanes degrees of mobility[82]

Having the same conformation as a real chain, polycatenanes possess the same degree of mobility with their common rotational, elongational, and rocking motions (Figure 1.11). [43] Polycatenanes can be either homocatenanes if the macrocycles are the same chemical unit, or heterocatenanes if the rings are different. [44] There are four main classes of polycatenanes based on how the rings link together (Figure 1.12). [45]

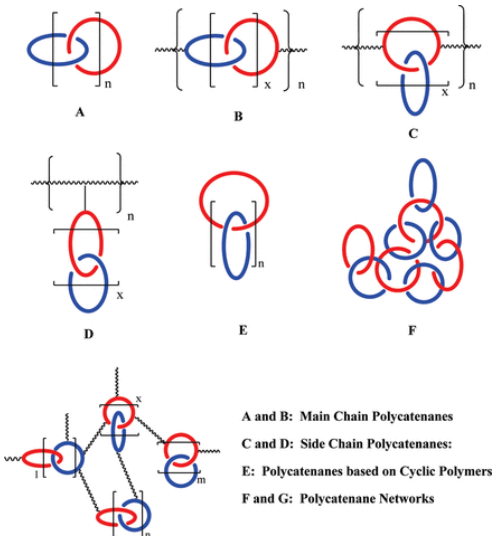

Figure 1.12: Polycatenanes classes[45]

The first class is given by Main Chain Polycatenanes. Belonging to this class are all the linear catenanes where the rings are one interpenetrated to the next one for a large number of units, or a series of "oligomers" not interlocked together but linked physically. Hydrogen bonds and π-π stacking are the main interactions between the rings. In the second class, there are the Side-Chain Polycatenanes, which are polycatenanes with two oligomers linked on the same ring or a ramification on the main backbone. This is achieved by placing a specific functional group on a macrocycle so that the ramification can be attached. The third class is polycatenanes based on Cyclic Polymers and as the name suggests are formed by the interpenetration of the macrocyclic ring and a cyclic polymer. The last class is represented by Polycatenane Networks of rings interlocked in more than one other ring and can cross-link with other networks.

The synthesis and characterization of a poly-[*n*]-catenane constitute a difficult step in the study of these materials. In this respect, Molecular Dynamic Simulation [46] is a useful tool for predicting conformational and constitutional properties so that the synthesis of the catenane can be designed in the best possible way. There are two synthetic approaches: the Statistical approach and the Template-Directed approach. The statistical approach is based on the stochastic closure ring on another, thus first the linear molecule threads inside one macrocycle, and then there is the cyclization. It is a highly inefficient method with a probability of 10^{-2} to synthesize the catenane, obtaining only small amounts of the compound. Moreover, the cyclization requires high dilutions but inhibits the elongation of the chain, as it is favored at high concentrations.

The template-directed approach [47] was introduced with the help of the host-guest chemistry. It is based on non-covalent interactions that allow placing the linear and macrocyling units to guide the interpenetration of the rings. Hydrogen bonds, hydrophobic interactions, π-π interactions, and metal ions coordination help the threading and preorganization before the cyclization. Thus, the system is controlled by the enthalpy leading to a high equilibrium constant and the reaction can be quantitative with yields up to 90%. For instance, there are examples of synthesis of [2]-catenanes by the template-directed approach that deepen the field of interlocking macrocycles, clarifying this kind of approach (Figure 1.13). [48]

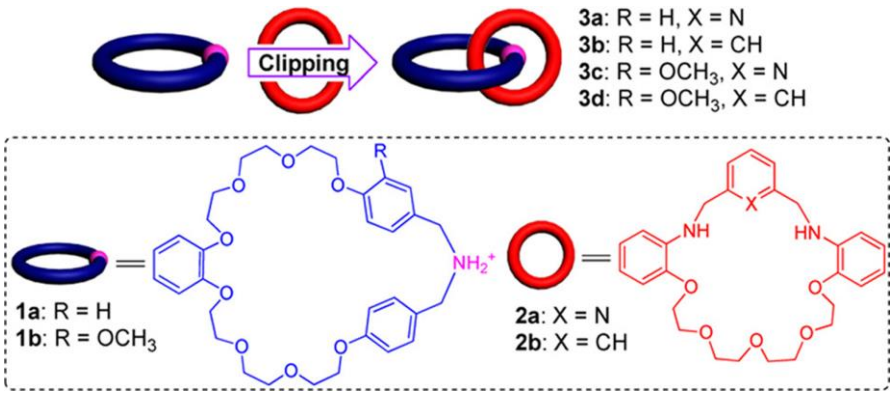

Figure 1.13: Example of template-directed approach[48]

Based on the kinetic or thermodynamic control of the reaction product yield and selectivity can be different (Figure 1.14). [49, 50]

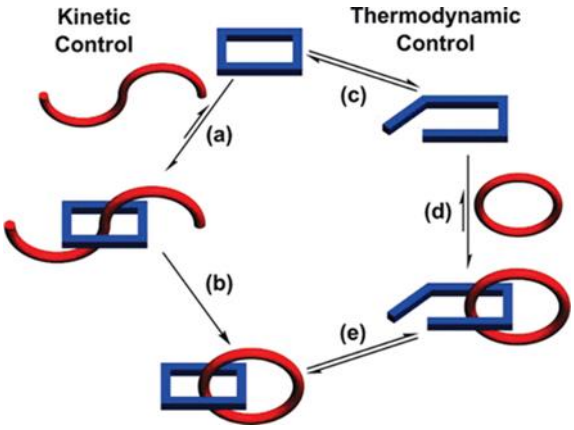

Figure 1.14: Kinetic and thermodynamic control in the catenane synthesis[49]

Generally, the kinetic product is obtained for short reaction times while the thermodynamic one is obtained for longer times. This is because the kinetic product is favored by irreversible reactions (or when the equilibrium is intensely moved to the right, *i.e.*, at the starting point of the reaction), and the thermodynamic one is for reversible processes where a proof-reading and error-checking process allows to break up covalent bonds or coordination bonds of the wrong assembled structures and thanks to the equilibrium form the most stable right structure. While the synthesis of oligo-[*n*]-catenanes with n<7 is already published and well known, [51, 52, 53] the production of large poly-[*n*]-catenane is still challenging and studied.

Poly-[*n*]-catenanes are rather recent studied compounds and the properties of these materials are not yet fully understood. The properties are related to the entire covalent, non-covalent, and mechanical bonds, the mobility of the chain, and the fraction of void inside the interpenetrated catenane, [54] that distinguish them from classical polymers. There are numerous ways in which catenanes [55] can be used and are mainly similar to MOFs applications, given common properties. I worked mostly on the porous ability of the compound, so I focused on molecules storage and isomers separations. Particularly, after some attempts with several molecules as guest inclusion, I tried some experiments for molecular recognition. I focused on the separation of the isomers of dichlorobenzene. These compounds can be present in wastewater and given their volatility can be air pollutants, with a high environmental impact. Moreover, dichlorobenzene isomers have high toxicity and

persistence. They are highly toxic with carcinogenic and mutagenic effects. They are widely used in the chemical industry, especially in organics and solvents synthesis, and are prepared by reaction of benzene with chlorine. A study of the separation of the three isomers *ortho*, *meta*, and *para*-dichlorobenzene is certainly useful. Thus, adsorption experiments were performed to see which isomer is retained the most and which is the structural behavior of the poly-[*n*]-catenane.

Apart from the above-mentioned examples, there are some applications that are different from the ones related to MOFs (catalysis, [56, 57, 22] biomedicals, [58] and so on) because are strictly related to the interpenetrated structure. Examples are applications in electronics, [59] where catenanes are used in conducting bridges and electronic devices, chemosensing, [60, 61] exploiting the designable receptors for anionic/cationic recognition and sensing, or even in molecular machines, [62, 63] based on mechanical-like movements as a result of external stimuli such as redox processes, pH changes or anionic/cationic interactions.

1.3 $[(ZnX_2)_{12}(TPB)_8]$ Poly-[*n*]-catenane: a case of study

Regardless of the difficulties of synthesizing large poly-[*n*]-catenanes, some examples of 1D interlocked catenanes are available. [64, 65] The cited article regards the synthesis of a poly-[*n*]-catenane using $ZnCl_2$ metal subunits and a trigonal ligand. The organic ligand used is 2,4,6-tris(4-pyridyl)pyridine (TPP) since previous works on MOFs or coordination networks were done using a very similar 2,4,6-tris(4-pyridyl)-1,3,5-triazine (TPT). [66, 67] The so formed catenane has been described as an interlocked chain of icosahedral cages. These interpenetrations are possible thanks to the π-π interactions between the central rings of the ligands. That said, regardless of the fact that ligand diversification can change the entire framework (this aspect will be addressed further in chapter 1.5) if the central pyridine of TPP is substituted with a simple benzene ring, that is 1,3,5-tris(pyridin-4-yl)benzene (TPB), the same structure should be formed. For this reason, the study of $[(ZnX_2)_{12}(TPB)_8]_n$ catenane was reported (X = Br, Cl, I). [68] First the Slow Crystallization method (see 3.2.1) using nitrobenzene as solvent was tried. The formed crystals were 0D nanocages of $[(ZnX_2)_{12}(TPB)_8]_{n*9}(C_6H_5NO_2)$. It resulted in an icosahedron structure having 12 faces open other than the 8 occupied by TPB. These cages are very large and can retain solvent molecules, both in an ordered and disordered fashion. The ordered molecules are the ones stacked to the walls due to efficient aromatic

interactions with the ligand. The disordered molecules have fewer interactions and are in the middle of the cage having high mobility being in a quasi-liquid phase. [69] The presence of ordered and disordered guests is justified by Thermogravimetric Analysis. Upon heating, first, the disordered one is released at lower temperatures, then the ordered guest due to the stronger host-guest interactions is released at higher temperatures. The effect of the solvent is fundamental as a templating agent for keeping the structure of the catenane in the crystalline phase.

Every cage is interlocked to each other through of π-π interactions forming 1D chains expanding along the c-axis. Individual chains interact with adjacent chains through hydrogen bonds between the H of the aromatic rings and the terminal ligand (*i.e.* chloride) of the metal salt. There is no continuity from one cage to the other suggesting a dynamic behavior is needed for the release and uptake of guest molecules (*i.e.* solvent).

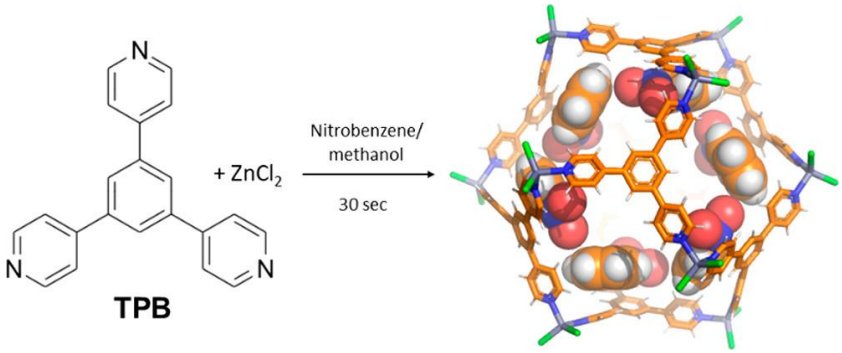

Figure 1.15: Fast Crystallization Synthesis[68]

For an improvement of the development of the material in view of potential applications, an attempt was made to synthesize it in such a way as to obtain a homogeneous product, in large quantities and in a short time using a Fast crystallization procedure (Figure 1.15). Without the error-checking process (*i.e.* due to the fast crystallization), the final product is only the $M_{12}L_8$ poly-[*n*]-catenane, rapidly synthesized thanks to the presence of large solvents (*e.g.* nitrotoluene, p-chlorotoluene, toluene, chlorobenzene) able to template it (small molecules like chloroform are not able to sustain the crystalline structure). The experimental results and the fitting of the diffraction pattern profile, confirms that the product is of high purity. Moreover, with Density Functional Theory calculations, the

interaction energies can be estimated, and it is possible to understand the stability of the monomer cage and the entire poly-[*n*]-catenane.

1.4 Toward green chemistry

The prospect of synthesizing the same polycatenane using a different technique, open to industrial scale-up, and saving solvents for economic and environmental benefits, is certainly attractive. The use of solvents in the chemical industry is becoming increasingly unsustainable, especially when it comes to non-recyclable, toxic, and fossil-based solvents. Among the 12 principles of green chemistry, there is one that states: "*The use of auxiliary substances (e.g. solvents, separation agents, etc.) should be made unnecessary wherever possible and, innocuous when used*". [70] Thus, it is useful to work with optimal use of solvents (when possible, with solvent-free reactions) [71, 72] depending on the whole life cycle of the product towards waste reduction and energy efficiency. Certainly, reactions in the liquid phase bring considerable advantages by influencing the dissolution of the reactants to initiate the reaction also controlling its equilibrium, and by acting as a heat transfer medium.

Besides the two kinds of polycatenane synthesis mentioned above, a synthesis without any templating guests has not yet been tried. For this reason, a mechanochemistry approach (*i.e.* neat grinding) has been chosen for a solid-state synthesis of the $M_{12}L_8$ poly-[*n*]-catenane. [73] According to IUPAC, a mechanochemical reaction is a "*Chemical reaction that is induced by the direct absorption of mechanical energy*" where "*Shearing, stretching, and grinding are typical methods for the mechano-chemical generation of reactive sites, usually macroradicals, in polymer chains that undergo mechano-chemical reactions*". [39] That is, by means of an external mechanical action that breaks some bonds, a chemical reaction is induced. [74] This definition does not imply that no solvent is present. In fact, in the general act of grinding, two types of reactions are possible and were performed during this study: LAG and NG. In a LAG experiment (acronym for Liquid Assisted Grinding), a small amount of a solvent (usually drops of it) is added to help the reaction (*i.e.*, as a catalyst) and template the structure. Once the poly-[*n*]-catenane, in an amorphous phase and good yields (more than 80%) was formed with LAG, an NG experiment (which stands for Neat Grinding) was tried, in this case no solvent at all was added.

A solvent-free experiment has some advantages both in the lab and industrial scale. First, there are no purification steps since the product is already pure enough and there is no solvent to be eliminated or recycled. Second, the reaction times are usually short, as it was proved that a sufficiently high purity poly-[*n*]-catenane can be synthesized within ca. 15 min of grinding.

Both at a lab and industrial scale the energy involved is significantly lower with respect to liquid-phase reactions. In the literature, there are also listed some drawbacks of this method but are mainly regarding the industrial field and could be solved with some engineering work. [75] For example, the handling of solid materials or heat-related problems due to exothermicity (like runaways) should be solved by designing proper reactors.

Grinding involves pressure and mechanical motion. [76] Both act at once for decreasing the free volume and increasing the rate of reaction. Also, the energy supplied enables particles and crystals to break up. Indeed, one of the main problems of grinding is the contact of the reactants, for a better course of the reaction, the particles size should be decreased in favor of the specific surface area. Besides the high concentration of the reactants, only the molecules with the right orientation on the surface of the particles take part in the reaction. After the formation of an intermediate compound, the final product is achieved with heat produced by the mechanical action and by the exothermicity of the reaction.

Having synthesized the poly-[*n*]-catenane and preparing it for several applications, it is useful to think about feasible future scale-up and see which are the offers the industrial sector can provide. In the laboratory, the grinding phase for preparing the amorphous sample is done with a pestle and a mortar. The industrial equipment is more complex and there are several devices, called mills, to be used (Figure 1.16). [76]

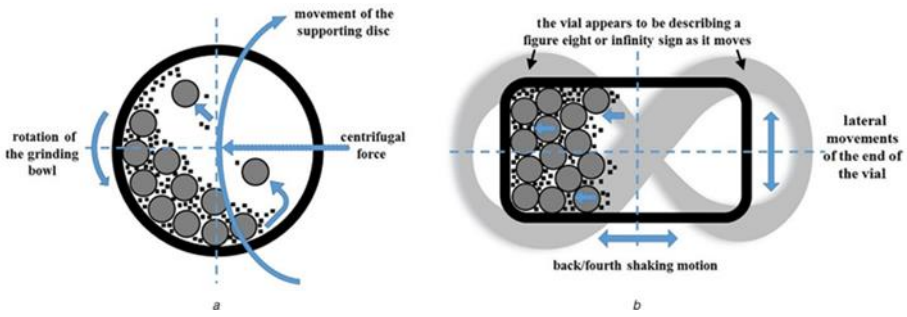

Figure 1.16: Ball Milling process[85]

There are mills where the particles collide with each other thanks to the push of solid plates or gas jets. Other works on the base of shear action where a shift of the reactants on a surface provides the mechanical action. At last, the most common mills are the Ball Mills which act with rotation and vibration exploiting both pressure and shear action for the operation. The shaking and planetary motions give some kinetic energy able to guarantee heat and mass transfer for the reaction to start (also the heat generated can start a slight melting of the particle surface and help the reaction) and is able to breakdown the particles to create new free surfaces able to react.

1.5 Ligand diversification

In the synthesis of a poly-[*n*]-catenane several parameters come into play. Both regarding the composition (solvent, pH, molar ratio, counter-ions…) and regarding the process conditions (temperature, pressure, time). [77] As far as composition parameters are concerned, there is one that is interesting to investigate. That is the ligand choice and its functionalization. As previously mentioned in chapter 1.3, small changes in the structure of the ligand can lead to major changes in the overall architecture of the final product. [78] For this reason, during this working period also the synthesis of several new ligands was investigated. Having TPB as the main backbone but with extra substituents so that we can use these ligands in the future and see the structural changes of any new catenanes from the original one already synthesized.

Organic ligands can have drastic effects depending on substituents, size, rigidity, geometry, and conformation. Metal salts and ligands both link each other as Lewis acid-base pairs. This choice of units is done on the so-called HSAB theory, which determines the formation of stronger or weaker links between organic and inorganic counterparts and thus the stability of the material. [79] The concept of HSAB theory is based on charge density, “Hard” species have high charge density while “Soft” species have a low one. The most stable and strongest bonds arise by the association of hard acids with hard bases or with soft acids with soft bases.

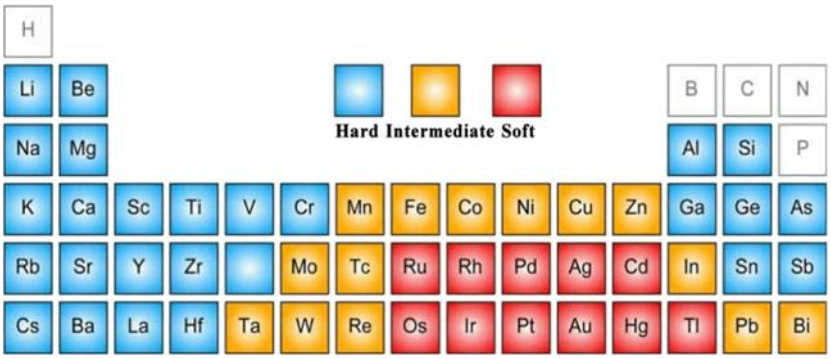

Figure 1.17: Hard, soft, and intermediate acids in the periodic table[86]

The entire periodic table can be classified into hard and soft (and even intermediate) acids (Figure 1.17) and depending on whether the ligand is a carboxylate (O donor), hence a hard base, or an azolate ligand (N donor), hence a soft base, one can design the most stable structure. This theory explains why TPB ligand (soft bases) can be linked efficiently with Zn^{2+} metal salts (intermediate acids). Stability is also given by the dimensions of the linkers and valence of the metal, smaller and more rigid ligands coupled with high-valence metals give a stable framework. Generally using long ligands favor the formation of ultra-large pores and promotes interpenetration rather than frameworks but affects negatively the whole stability favored instead by rigid and dense ligands. To compensate for the stability, one should increase the number of connections between ligand and metal SBU.

Considering the TPB as the main structure the insertion of a substituent on one (or more) pyridines can not only modify the polarity but also the torsional angle of the pyridine with respect to the central benzene and therefore its symmetry. Every group has proven effects. Amino groups are specifically used as a point of linking even for post-synthetic modifications. Methyl groups block the water from attacking the metal subunits thanks to their hydrophobicity thus increasing the stability in aqueous solutions. Halide groups directly influence polarity. Hydroxyl, C≡C, and C≡N groups, thanks to the possibility of establishing Van der Waals interactions and hydrogen bonds, can enhance the host-guest connections. [80]

The insertion of some of these groups on the ligand part of the catenane has also been developed and will be dealt with in this thesis.

2 Results and discussions

2.1 Mechanochemical synthesis

For the reasons described in section 1.4, the synthesis of $M_{12}L_8$ poly-[*n*]-catenane via mechanochemical synthesis was investigated. First, Liquid Assisted Grinding experiments were performed with zinc bromide. Thus 30 mg of TPB and 34 mg of $ZnBr_2$ were grinded for 15 minutes in a mortar with 5μL of methanol (Figure 2.1).

Figure 2.1: Mechanochemical synthesis of a1 phase [73]

The obtained powders were analyzed by powder X-ray diffraction method. In the early experiments' patterns there were some peaks from TPB unreacted, as can be seen comparing the diffractograms with the commercial (Figures 2.2a and 2.2b) TPB PXRD pattern. Specifically, the peaks at 2θ/° *ca.* 9, 16, 18.5, 20, 22, 24. For this reason, an excess (30 mg) of metal salt was added to the previously measured powder, grinded some more, and again tested at PXRD. The new diffraction diagram is free of the characteristic peaks leaving only an amorphous phase (**a1**) pattern with two main "bumps" or "broad peaks" as can be seen in Figure 2.2c.

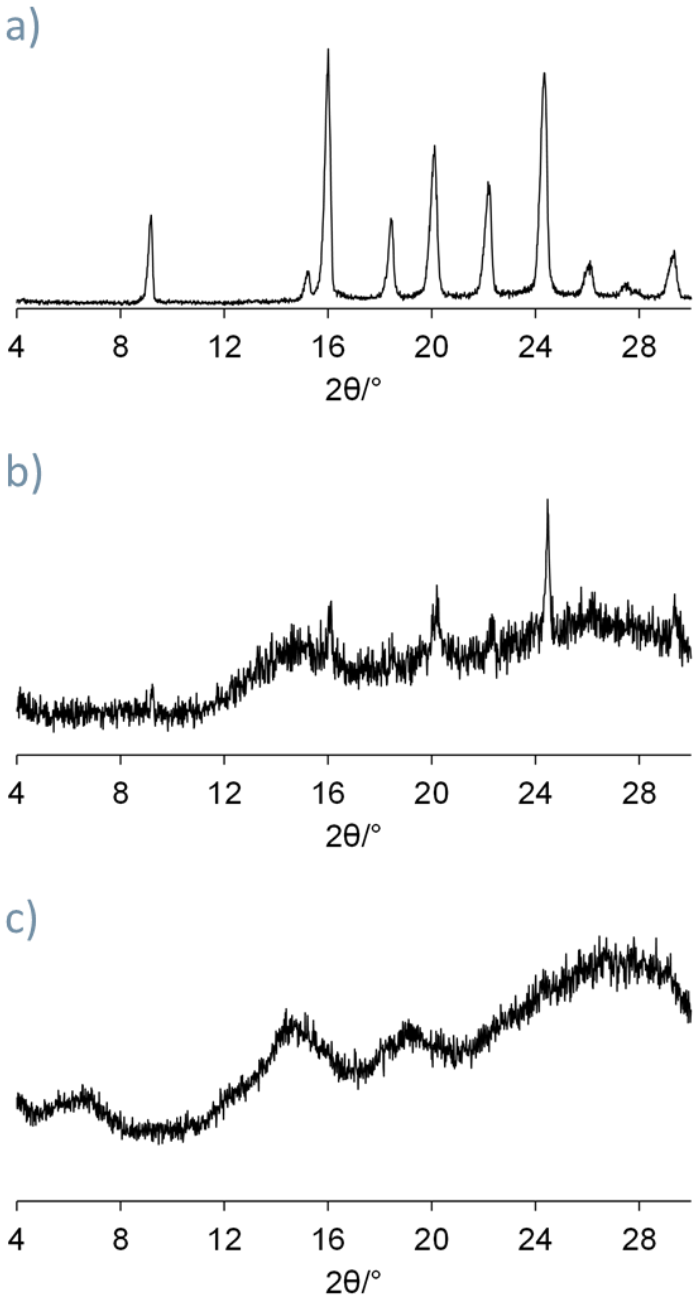

Figure 2.2: PXRD patterns of a) commercial TPB, b) a1 phase with unreacted TPB, c) a1 phase

The methanol added should help the solid-state reaction and thermogravimetric analysis was done to find that a small amount is present inside the final product.

The study of the structure could not be done in the amorphous phase, thus the grinded material was immersed in a solution of 1,2-dichlorobenzene overnight, hoping that the solvent molecules would enter (templating effect) the alleged structure and swell the catenanes so that they stack together and give a crystalline phase (**c1**) possible to be characterized by powder XRD. An amorphous to crystalline transformation (**a1** to **c1**) occurred as can be seen from the diffraction pattern (Figure 2.3).

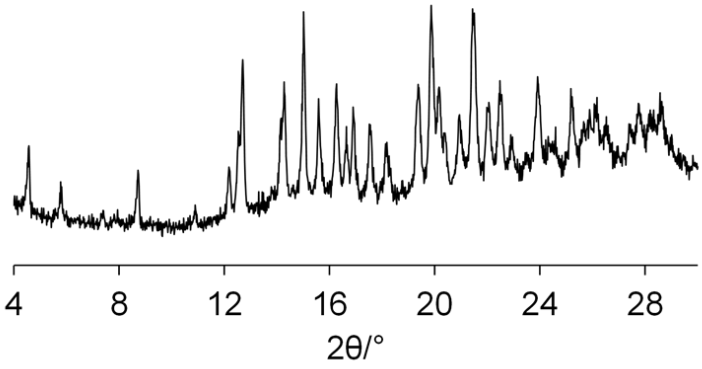

Figure 2.3: PXRD pattern of c1 phase

TG analysis, shown in Figure 2.4, confirmed the presence of 1,2-dichlorobenzene inside the poly-[*n*]-catenane in a sufficient quantity (24.1%). The TGA and crystalline PXRD characterization confirm the formation of the $M_{12}L_8$ poly-[*n*]-catenane.

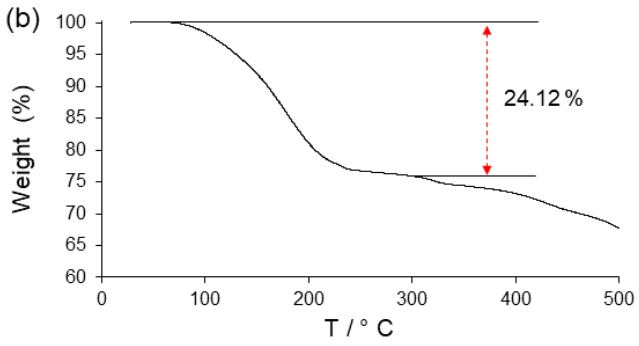

Figure 2.4: TG analysis of crystalline phase[73]

However, the amorphous to crystalline transformation does not always occur using only 1,2-dichlorobenzene. Instead, when the amorphous compound **a1** is immersed in a mixture of methanol and 1,2-dichlorobenzene, the transformation always takes place. This suggests that the presence of methanol is essential and could explain the possible dynamic behavior of the catenanes. Methanol is small and can enter the cages but does not have a strong enough template effect (*i.e.* is not aromatic) and, due to its high volatility, it will not stay long enough inside the cages. Conversely, 1,2-dichlorobenzene, is substantially bigger than methanol and depending on the structure of the amorphous phase, might not enter the cages and template the entire poly-[*n*]-catenane architecture. Methanol, with its smaller size, can enter the cages, open them up and let the 1,2-dichlorobenzene enter which then is large enough to template the poly-[*n*]-catenane by π-π interactions making the material crystalline.

After LAG experiments, the next step was studying the grinding without solvent. Thus, TPB and metal salt in excess were grinded in a mortar. The PXRD analysis showed that the sample was amorphous (Figure 2.5a), while elemental analysis confirmed the ratios and general formula. Again, if the compound is immersed in a 1,2-dichlorobenzene/MeOH (5 mL : 1 mL) solution, an amorphous to crystalline transformation occurs (Figure 2.5b).

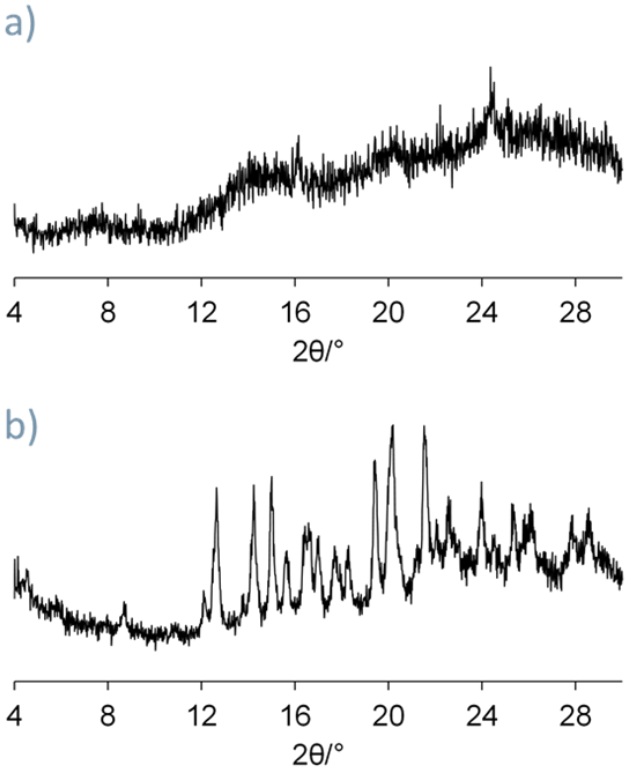

Figure 2.5: PXRD patterns of a) a1 phase from NG, b) c1 phase

One could object that the morphology could be made up of oligo-[*n*]-catenanes instead of poly-[*n*]-catenanes as commonly seen in catenane synthesis. Besides the fact that the solid does not dissolve in a 1,2-dichlorobenzene solution, suggesting the presence of a polymeric phase, to be sure and exclude this possibility, IR analyses were conducted. For a complete study, the IR spectra of TPB, 1,2-dichlorobenzene, amorphous solid **a1**, and crystalline solid **c1** were measured and analyzed (Figures 2.6 and 2.7). First, the TPB spectrum presents three main peaks at 1591 cm^{-1} with a shoulder at 1608 cm^{-1}, 814 cm^{-1}, and 611 cm^{-1}.

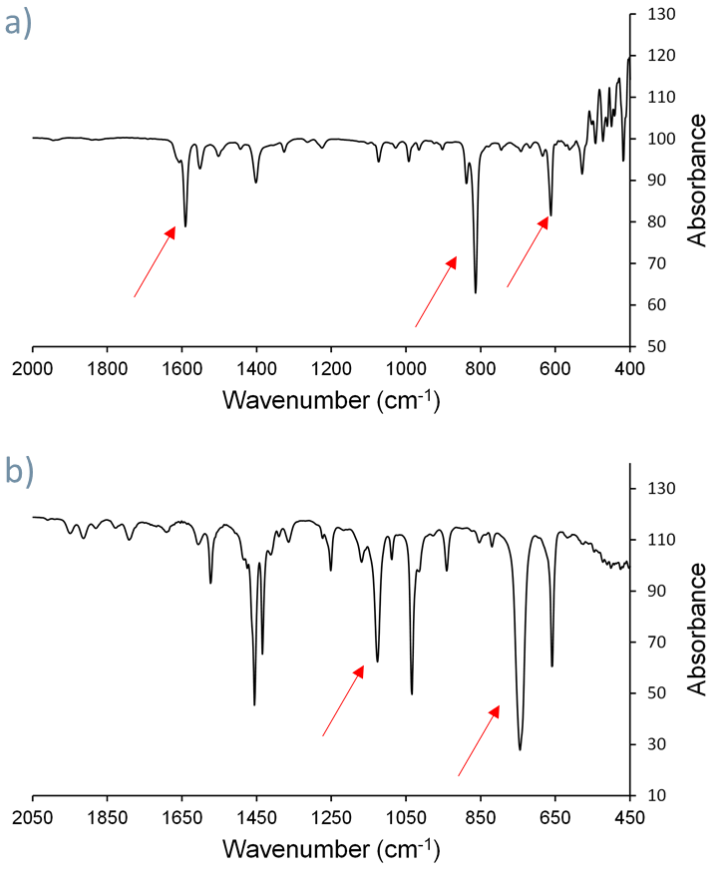

Figure 2.6: IR spectra of a) commercial TPB, b) 1,2-dichlorobenzene

These peaks are referred to as the vibrations and scissoring of the C-C and C-H bonds of the aromatic rings crystalline. Both, crystalline and amorphous phases show characteristic TPB peaks corresponding to unreacted TPB. In the crystalline phase, there are also peaks in common with the 1,2-dichlorobenzene spectrum like

the ones at 750 and 1124 cm^{-1}. Finally, as proof that the poly-[*n*]-catenane is formed also in the solid-state, there are peaks in common to the crystalline phase and the amorphous one, like the ones at 1614, 1030, 815 cm^{-1} and particularly the one at 634 cm^{-1} which is reported to be characteristic of the vibration of the bonds of the pyridine-Zn metal complex.

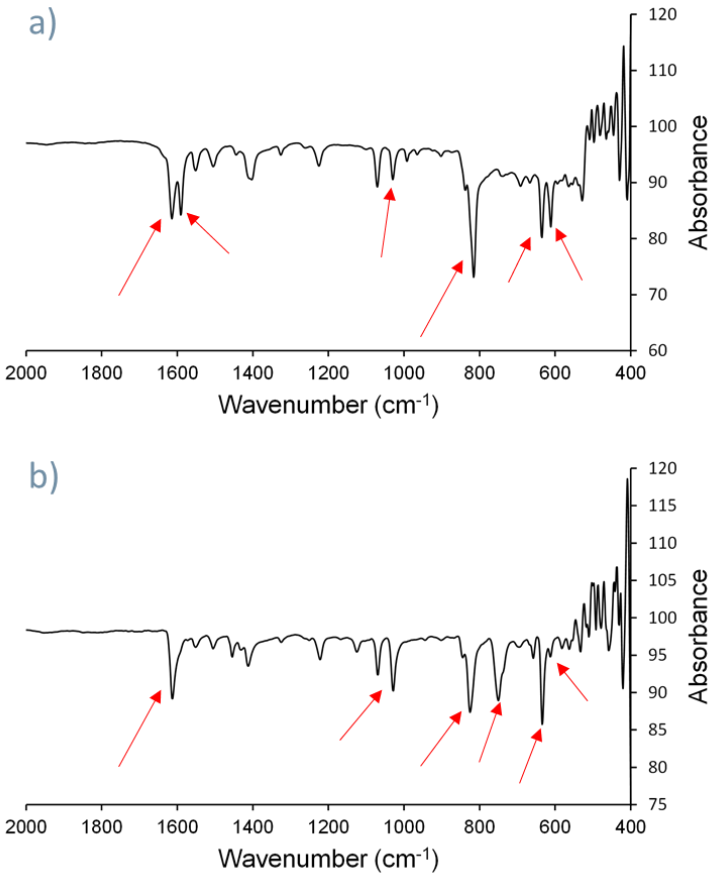

Figure 2.7: IR spectra of a) a1 phase, b) c1 phase

In order to gain some structural information from the amorphous phase, one TPB + $ZnBr_2$ grinded sample and a sample prepared by instant synthesis were prepared and analyzed by Solid-State NMR analysis. The results are illustrated in Figures 2.8, 2.9, and 2.10. In the first spectra (Figure 2.8) the quaternary and non-quaternary carbon atoms of the TPB are shown. When it is grinded with the metal salt to form the poly-[*n*]-catenane there is a shift (Figure 2.9) in these peaks due to electronic reasons and π-π interactions of the benzene rings. Comparing the crystalline **c1** to the amorphous phase **a1**, one can see a decrease in the intensity of the characteristic

benzene and pyridine peaks (Figure 2.10). This decrease is due to a loss of mobility both in the pyridine and in the benzene, pyridines which have a more dynamic behavior with respect to benzenes that take part in π-π interactions (*i.e.* sort of stabilization). Moreover, there are the peaks of 1,2-dichlorobenzene, very defined and intense, a sign of its great mobility.

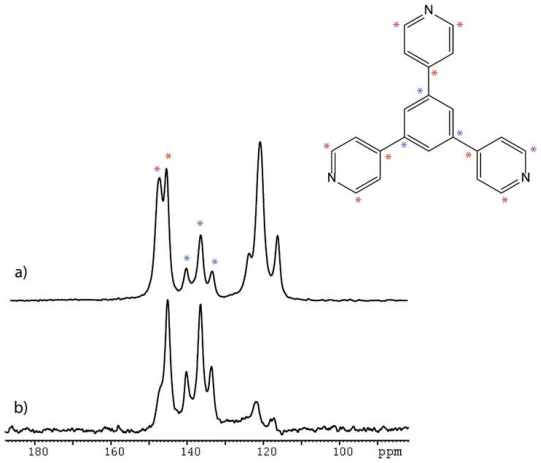

Figure 2.8: a) CP/MAS ^{13}C solid state NMR spectra of the ligand TPB, b) CP/MAS ^{13}C solid state NMR with non-quaternary suppression [73]

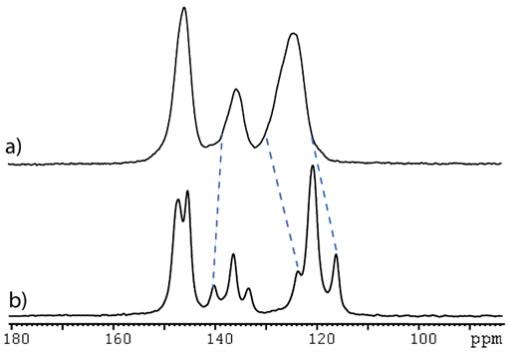

Figure 2.9: CP/MAS ^{13}C solid state NMR spectra of a) a1 phase, b) TPB [73]

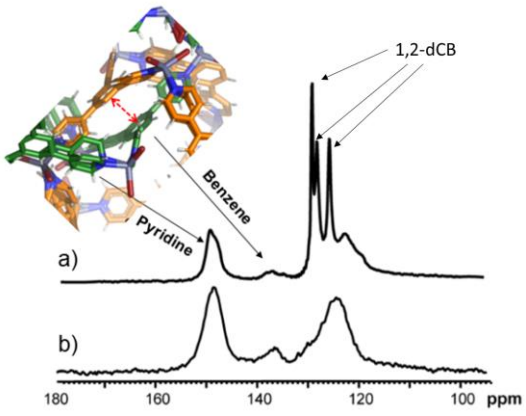

Figure 2.10: HPDec/MAS ^{13}C solid state NMR spectra of a) a1 phase, b) c1 phase [73]

Clearly, the $M_{12}L_8$ poly-[*n*]-catenane has lots of potentialities, some of which we have been studying and will be discussed in the following section. As mentioned in the introductory chapter, mechanochemical synthesis tries to follow the rules

dictated by the twelve principles of green chemistry. In this respect, the very first point suggests waste prevention, to prefer the reuse with respect to the cleaning process of waste. In this perspective, the material discussed here provides a viable alternative following its use and not simply treating the product as a non-reusable waste.

It was discovered that if the compound is left immersed in water for 2 days, the poly-[*n*]-catenane structure completely disintegrates. The coordination bonds between the zinc and the nitrogen, that keep the whole structure assembled, break up. While the metal salt dissolves in water, the solid part is constituted only by the ligand TPB. Upon filtration of this suspension and PXRD analysis, it was found that the diffraction pattern matches that of the commercial TPB (Figure 2.11). Actually, since the pattern is the same, it means that the white solid powder is a very pure TPB. This means that with this process, the contaminated water can be sent to purification, while the white solid, once dried, can be utilized again for the preparation of new material. This can be done again and again to prevent waste and for the good of the circular economy.

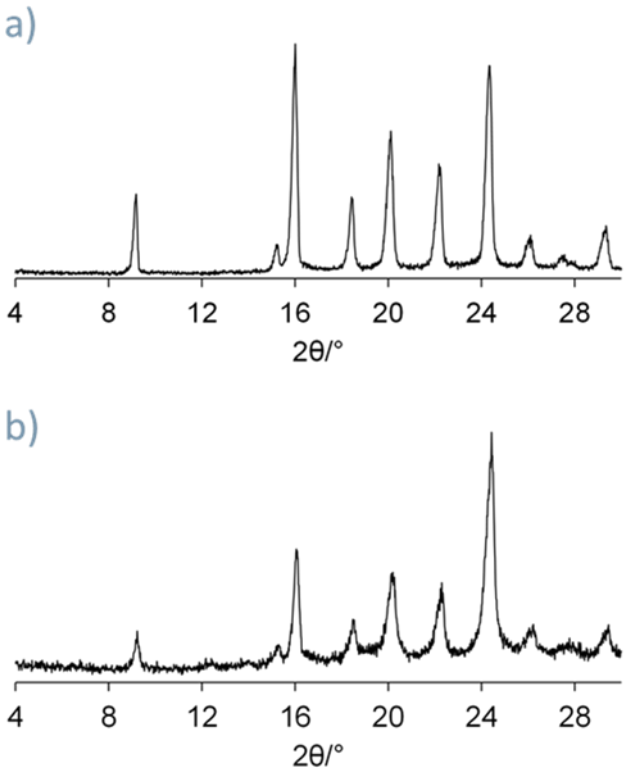

Figure 2.11: PXRD pattern of a) commercial TPB, b) TPB recycled from poly-[*n*]-catenane

2.2 Applications

2.2.1 Molecular storage

The study of the $M_{12}L_8$ poly-[*n*]-catenane for its potential applications was based on its porosity given the great internal volume of the cages able to reach up to 2600 $Å^3$. Several templating solvent molecules have been tested for storage. On the basis of the first TPB poly-[*n*]-catenane, [73] where the included solvent was nitrobenzene, another aromatic molecule such as 1,2-dichlorobenzene was used. First, TPB and zinc bromide were dissolved in 1,2-dichlorobenzene and subjected to an instant synthesis experiment, producing great crystalline products as seen by the corresponding PXRD diagram. The crystalline pattern is very similar to those reported with some shifts due to the different solvents. This indicates that the synthesized crystalline solid is isostructural to those obtained with different aromatic guests. As mentioned also in the Introduction, the presence of methanol can only help the entrance of the 1,2-dichlorobenzene molecules inside the cages. The presence of 1,2-dichlorobenzene was confirmed also with IR analysis.

Tested with $ZnBr_2$, it was interesting to change the counter-ions of the metal salt to see if there was any change in the final structure and if it was formed. Experiments with $ZnCl_2$ and $ZnBr_2$ were carried out (see 3.2.1, Fast Crystallization) to explore if the instant synthesis yields the same structure as that of the $ZnBr_2$ poly-[*n*]-catenane. Upon filtration of the solid, both the chloride and iodide product generated a crystalline phase according to the PXRD pattern. Comparing the three diffraction patterns of the crystalline phases prepared from each of the three metal salts, one can see that there are some differences in crystallinity (Figure 2.12). Evaluating the intensity of the peaks and the trend of the overall pattern, it can be figured out that the $[(TPB)_8(ZnCl_2)_{12}]$ and $[(TPB)_8(ZnBr_2)_{12}]$ poly-[*n*]-catenanes give the most crystalline pattern with respect to the $[(TPB)_8(ZnI_2)_{12}]$ which has a very poor crystallinity.

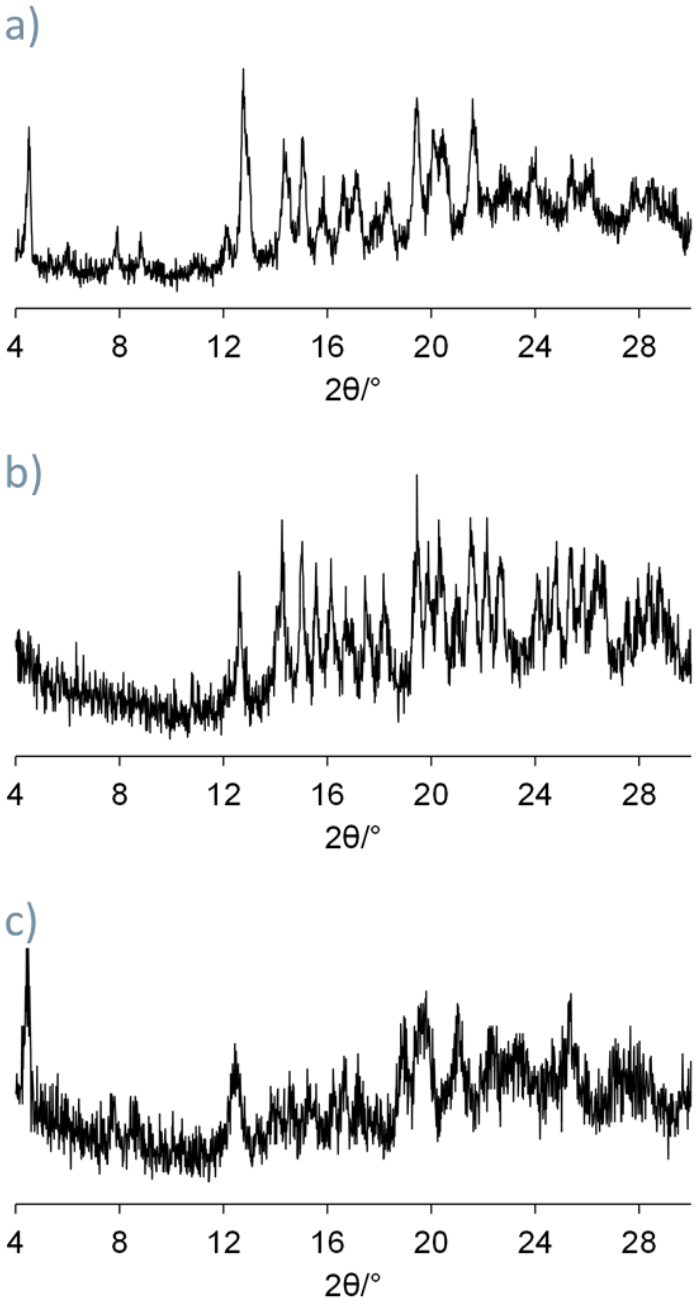

Figure 2.12: PXRD pattern of instant synthesis experiments using a) $ZnBr_2$, b) $ZnCl_2$, c) ZnI_2

Even if this is not yet confirmed, it should be related to the differences between the three halogens along the periodic table. The size decrease going from iodine to bromine to chlorine while the electronegativity follows the opposite course. In this

way we can assume that chlorine is more reactive than bromine which is more reactive than iodine both for steric and electronic reasons, making the zinc able to form stronger and more stable bonds in the whole structure of the poly-[*n*]-catenane, favoring the packing and thus the crystallinity. In particular, the electrostatic interactions among the 1D chains of linked $M_{12}L_8$ cages might show different strengths (*i.e.* stronger in the $ZnCl_2$ and weaker in the ZnI_2) leading to different lattice energies. Current work is being carried out by means of DFT calculations to gain insights into this topic.

Thermal stability

An ex-situ thermal analysis of the compounds can account for the differences between metal salts highlighting the changes in the patterns. In this way, three instant synthesis samples were prepared as usual at room temperature and then put in the stove for 4 hours at constant temperature starting from 150 °C. Then the sample is cooled down and analyzed by PXRD. This routine is repeated by gradually increasing the temperature (10 °C at a time) until 270 °C. The results obtained are shown below pointing to the crystalline or amorphous behavior (Table 1).

	TPB+$ZnBr_2$	TPB+$ZnCl_2$	TPB+ZnI_2
150 °C	**Am**	**Am**	**Am**
170 °C	**Am**	**Am**	**Am**
190 °C	**Am**	**Am**	**Am**
200 °C	**Am**	**Cr**	**Am**
210°C	**Am**	**Cr**	**Am**
220 °C	**Am**	**Cr**	**Am**
230 °C	**Cr**	**Cr**	**Am**
240 °C	**Cr**	**Cr**	**Am**
250 °C	**Cr**	**Cr**	**Am**
260 °C	**Cr**	**Cr**	**Am**
270 °C	**Cr**	**Cr**	**Am**

Table 1: Thermal stability trend (Am: Amorphous, Cr: Crystalline)

It is interesting to see that after the crystalline phase is annealed for 4 hours at 150 °C, it becomes amorphous for each of the metal salt species. At this temperature, the solvent included in the interpenetrated $M_{12}L_8$ cages is released, and there is no templating effect causing the amorphization of the material. Furthermore, at some point, there is the formation of a new crystalline phase (**c2**).

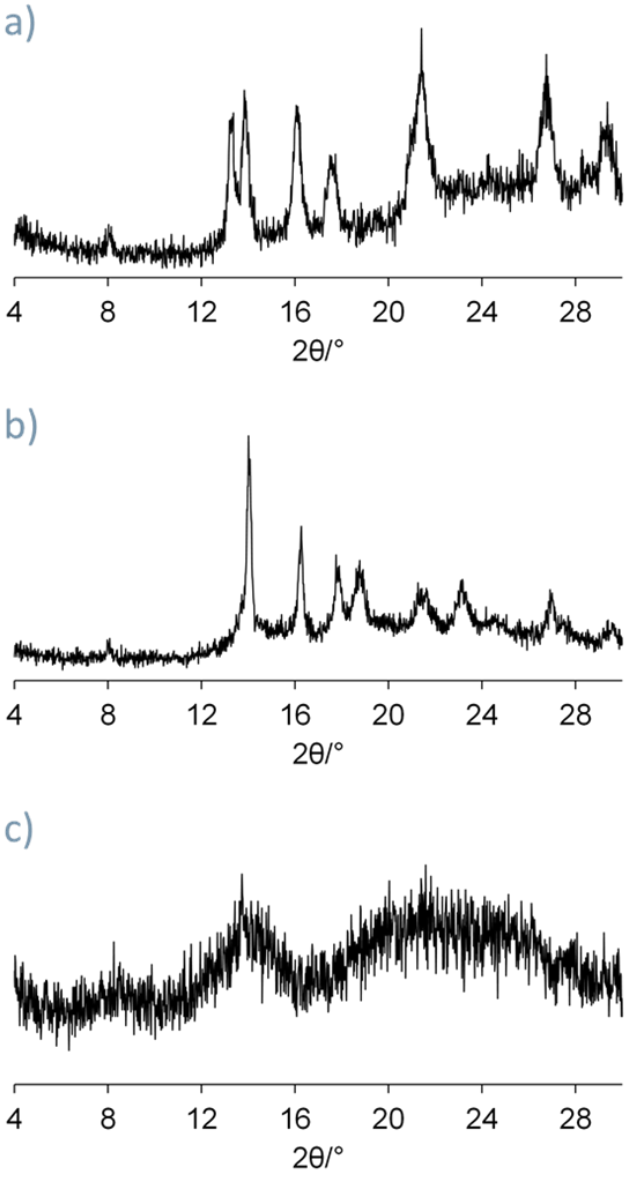

Figure 2.13: Thermal analysis experiment, PXRD pattern of a) bromide experiment at 240°C, b) chloride experiment at 200°C, c) iodide experiment at 270°C

The reason why this amorphous to crystalline transformation (**a1** to **c2**) occurs at different temperatures depending on the metal used could be the same described above. Thus, the chloride salt, more prone to create stable structures, forms the new crystalline phase at 200 °C (Figure 2.13b). Following this, the bromide salt starts at 230 °C to become crystalline because needs more energy, with respect to other, to achieve this phase, reaching a peak of crystallinity around 240 °C (Figure 2.13a). Both the chloride and bromide compounds keep their crystallinity until the maximum temperature of 270 °C, just decreasing in quality as the temperature increases. Instead, with the iodide salt, no transformation occurred at all (Figure 2.13c). This could mean that either the material requires more energy, and it needs to reach a higher temperature, or the weak interactions with zinc iodide prevent the formation of this new crystalline phase upon heating. It is interesting to note that, after a series of experiments, the dynamism of phase **a1** has been demonstrated. Indeed, the amorphous phase generated following heating, once immersed in a mixture of 1,2-dichlorobenzene and methanol, undergoes a transformation to the previous crystalline phase **c1**.

Further solvents

Other solvents were used in the instant synthesis experiment to see the dynamic behavior in presence of various guests. Toluene and para-chlorotoluene showed the formation of a very similar crystalline phase with the main difference in the shift of peaks (Figure 2.14a and Figure 2.14b). Choosing a different type of solvent like chloroform, the pattern changes. Like methanol, chloroform is a small molecule, with respect to the aromatic species used till now, and can enter the cages but is volatile and is not able to give rise to interaction strong enough to recreate the crystalline phase of the poly-[*n*]-catenane (Figure 2.14c).

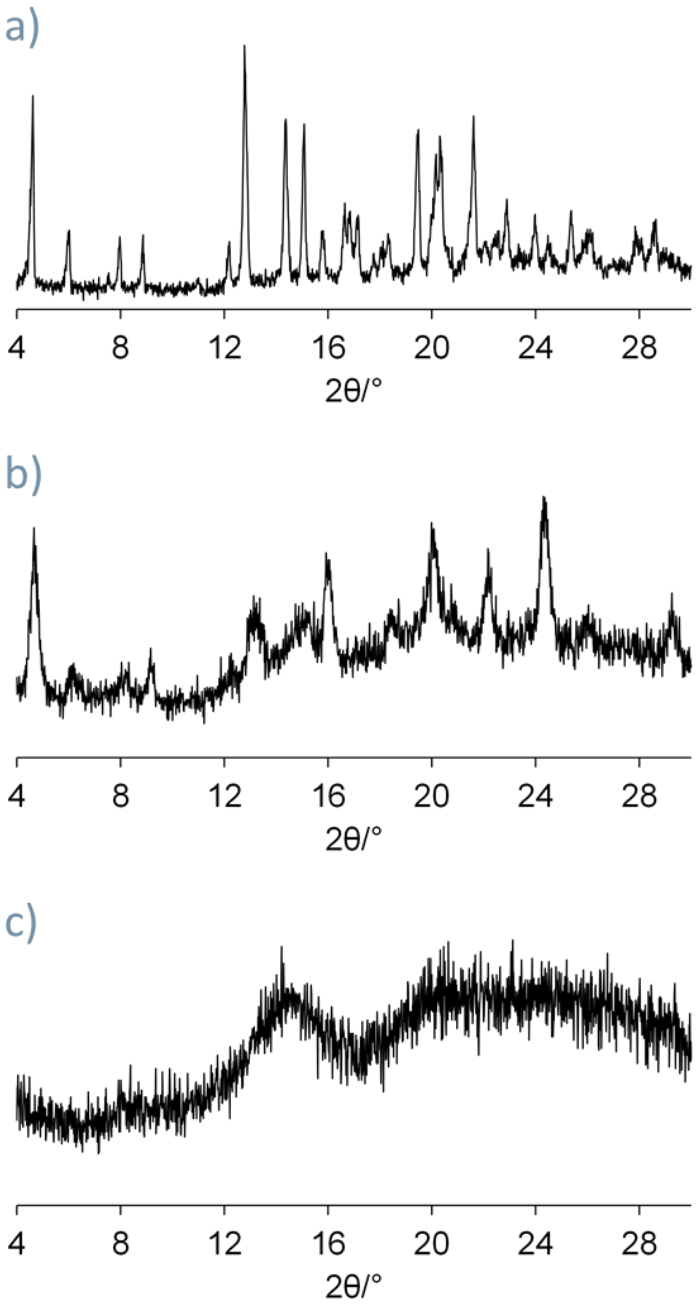

Figure 2.14: PXRD patterns of instant synthesis experiments using a) p-chlorotoluene, b) toluene, c) chloroform

With a view to using this material for drug storage and delivery, also paracetamol was tried, due to the presence of an aromatic ring in the structure. Thus, both paracetamol and its precursor, *para*-aminophenol, were used as solvents in instant

synthesis experiments. Unfortunately, neither resulted in a crystalline structure, probably due to their size and the presence of several functional groups. Nevertheless, more work will be needed in this direction, for instance trying very concentrated solutions of guest molecules like 1:100 TPB:guest ratio.

Alcohols like methanol, ethanol, propanol, and butanol were tried as guests to see if induced the amorphous-to-crystalline transformation. It has been seen that upon immersion of the amorphous phase for all of the alcohols mentioned, crystalline phases were obtained. The powder XRD pattern indicates that is the catenane. Due to their low boiling point, while the PXRD experiment is running, the guest goes away, as the crystalline phase gradually turned amorphous. One might therefore think that by using alcohols with longer chains, and a higher boiling point, this phenomenon can be avoided. Unfortunately, the experiments performed with 1-heptanol, 3-nonanol, and 1-heptadecanol could not confirm this theory. Indeed, when the amorphous solid, prepared by ball milling, is immersed in a 6 mL solution of heptanol or nonanol (in both cases it is a very high concentration with respect to TPB) a completely amorphous solid is generated. One explanation can be that there are not enough host-guest interactions. The same applies when immersing the amorphous **a1** in a solution of 50 mg of heptadecanol in 5 mL of MeOH obtaining still an amorphous phase. A reason for this last case could be that the amount of alcohol is not enough (the ratio used is just 1:2 TPB:heptadecanol) for the templating effect. However, further studies must be conducted.

2.2.2 Isomer recognition

Having tested 1,2-dichlorobenzene and as mentioned above, being able to use this material for isomer recognition, it was natural to try to see how it behaves in the presence of 1,3-dichlorobenzene and 1,4-dichlorobenzene. By means of fast synthesis methods, using 1,3-dichlorobenzene the crystalline phase is formed with each metal salt (Figure 2.15a). On the contrary, with 1,4-dichlorobenzene dissolved in chloroform due to its solid nature, the amorphous phase is formed upon fast synthesis (Figure 2.15b). Instead, by immersing an amorphous catenane sample in 1,3-dichlorobenzene or 1,4-dichlorobenzene for several days, the result was an amorphous phase in both cases. Experiments were carried out in which a sample of amorphous phase **a1** was immersed in a mixture consisting of 28.5 mg of 1,4-dichlorobenzene dissolved in methanol (TPB:1,4-dCB ratio = 1:2). Stirring times

were also up to one week. Once the mixture was filtered and allowed to dry, it was amorphous. With regard to 1,3-dichlorobenzene, the amorphous sample **a1** was immersed in 6 mL of 1,3-dCB (TPB ratio: 1,3-dCB = 1:0.5).

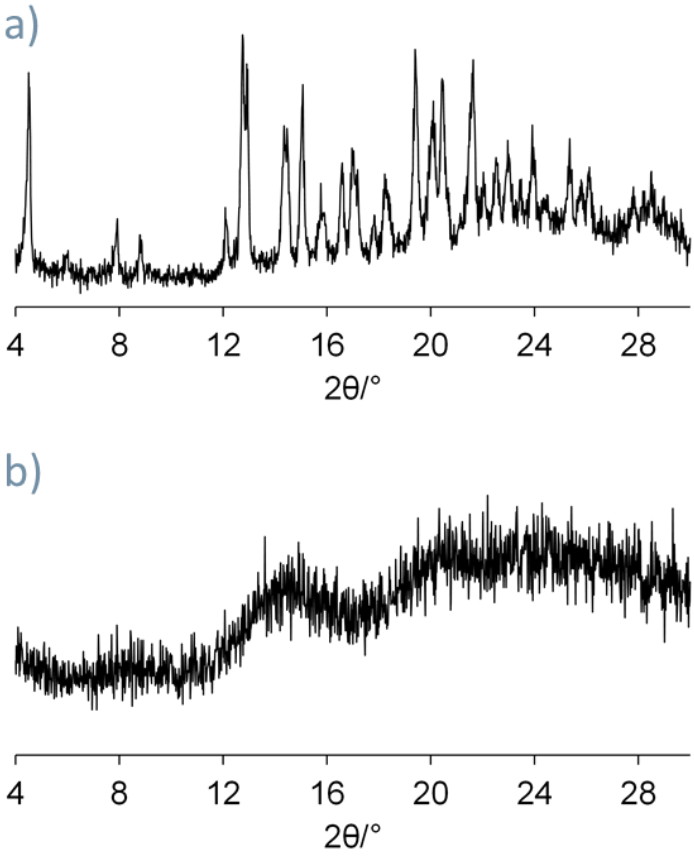

Figure 2.15: PXRD patterns of instant synthesis experiments using a) 1,3-dichlorobenzene, b) 1,4-dichlorobenzene

Seen the results, the amorphous-to-crystalline transformation seemed a powerful tool to identify and possibly separate the isomers. Mixtures of the isomers were prepared and the amorphous poly-[*n*]-catenane was immersed in the solution, stirred for one or more days then filtered and measured with PXRD analysis. A mixture of 1,2-dichlorobenzene and 1,4-dichlorobenzene in a 1:1 ratio, was prepared. 2 mL excess of 1,2-dichlorobenzene had to be added to completely dissolve the solid 1,4-dichlorobenzene. The solid, after immersion, resulted to be crystalline (Figure 2.16b). This outcome was found for each metal Cl, Br and I with

a crystallinity decreasing in this order, probably for the reasons explained in the previous section.

A mixture of 1,2-dichlorobenzene and 1,3-dichlorobenzene in a 1:1 ratio was prepared. The results were the same as the previous set of experiments, with a crystalline pattern (Figure 2.16a). The consequence of this is that 1,2-dichlorobenzene is certainly inside the poly-[*n*]-catenane, giving it the typical crystalline phase. This topic will be further explored as, by solid-state NMR analysis, there is some evidence that in the cages can be present a mixture of the two solvents.

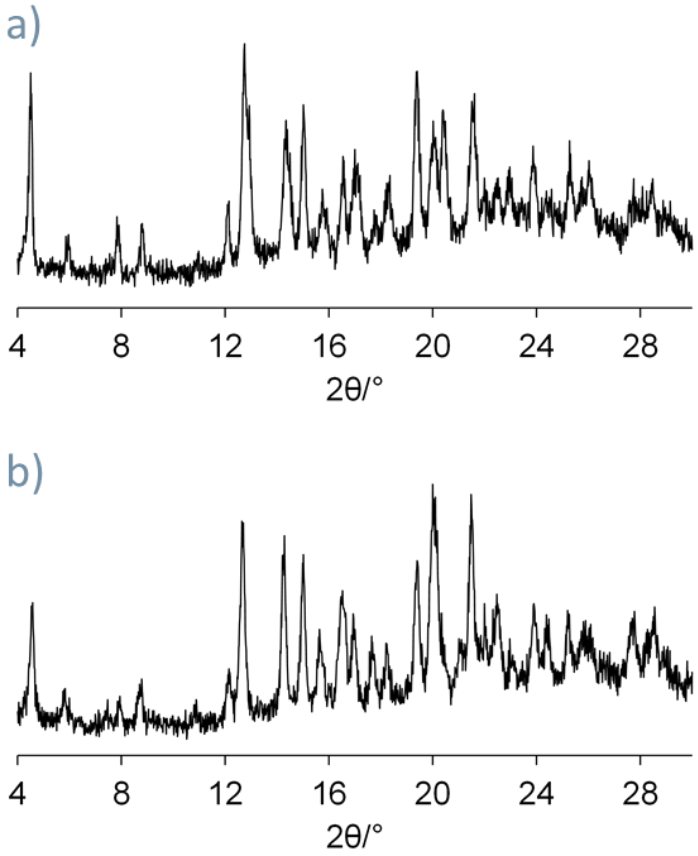

Figure 2.16: PXRD pattern of adsorption test using a) 1,2-dCB+1,3-dCB mix, b) 1,2-dCB+1,4-dCB mix

The last experiment raises an interesting question.

If the template effect that generates the crystalline phase is due to π-π interactions of the aromatic solvent ring with the ligand in the scaffold, why shouldn't the *meta-* and *para-* isomers have the same effect as the *ortho-* one?

To answer this question, calculations had to be carried out to establish the exact amount of 1,4-dichlorobenzene that should go into a certain amount of catenanes. It resulted that the ratio dichlorobenzene:TPB should be much higher with respect to the ones previously mentioned. To this end, 1.3 g of 1,4-dichlorobenzene was dissolved in 15 mL of methanol. After immersing the amorphous catenane sample in it, the filtered solid was found to be very crystalline (Figure 2.17). The sample was tested after three weeks at ambient conditions and showed the same good crystallinity indicating that the guests inside the nanocages are stable.

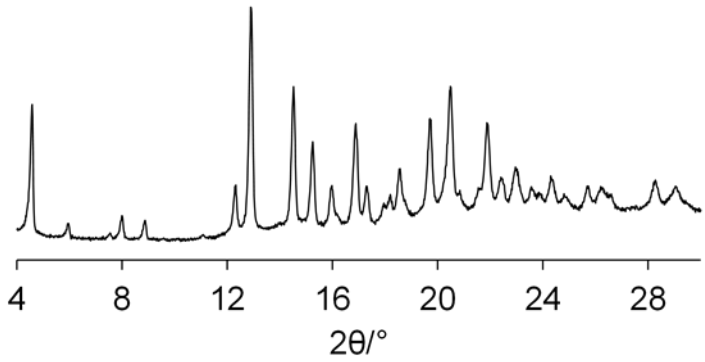

Figure 2.17: PXRD pattern of instant synthesis experiment using 1,4-dichlorobenzene

With this result, it is necessary to rethink the behavior of the various isomers in order to optimize their possible separation and it opens doors to future studies. One of these could take advantage of the different interactions with the material to be able to design a kind of chromatographic column. In this way, the exact amount of material to be used to separate a certain volume of the mixture of the three isomers is calculated, the column is packed with the catenane, prepared by grinding or by fast synthesis, and finally, the analyte mixture is loaded. This, gravimetrically or aided by gentle pressure, percolates through the column and the three isomers may separate from each other.

2.3 Diversification

As described in the introduction, the study of the stereoelectronic properties of the organic ligand is of fundamental importance for the tuning of both structural and functional properties of the MOF.

The interest in substituted ligands led us to study an optimal synthetic pathway for the synthesis of a small library of differently functionalized TPB derivatives. After literature research, it was considered that the best and most straightforward way was via a Suzuki-Miyaura Coupling. [81] This is a very commonly used reaction to create carbon-carbon bonds. It involves the reaction of an aryl boronic ester with an aryl halide catalyzed by a palladium species in the presence of an aqueous base (*i.e.* KOH).

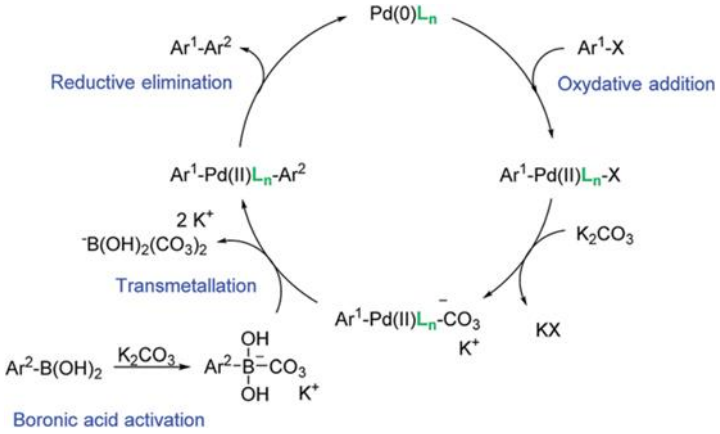

Figure 2.18: Suzuki-Miyaura Coupling cycle[84]

The entire process constitutes a catalytic cycle (Figure 2.18) where the Pd(0) species is oxidized to Pd(II) and create an intermediate with the aryl halide. Depending on the strength of the Ar-X bond this intermediate is created more or less easily according to the trend Ar-I>Ar-Br≥Ar-OTf>>Ar-Cl≈ArOTs. Then the aryl boronic ester takes part forming an Ar-Pd-Ar' intermediate. Ultimately the C-C bond is formed via a reductive elimination reaction to give Ar-Ar' and regenerating the catalytically active Pd(0) species. The presence of a base is essential, for the activation of the boronic acid through the formation of the corresponding "ATE" specie.

The starting point was to synthesize the TPB as such (compound **2**), without any substituent group. The first step begins with 1,3,5-tribromobenzene by reacting it

with 3 equivalents of pyridine boronic ester (compound **1**) to be sure all the three bromines would react (Figure 2.19).

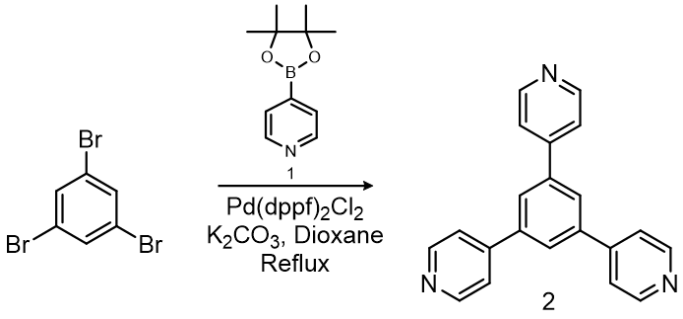

Figure 2.19: Synthesis of 1,3,5-tri(pyridin-4-yl)benzene (**2**)

After the work-up of the reaction and a flash chromatographic column purification, the white solid obtained was characterized by NMR and GC-MS analysis and compared with the respective patterns of the commercial TPB (Figure 2.20). The NMR spectrum reflects the entire symmetry of the molecule, showing the 2 doublets of the 12 hydrogens on the pyridines and one singlet of the 3 hydrogens on the central benzene. Having synthesized compound **2** just in search of the optimal reaction conditions, it was not purified, and the NMR spectrum shows some additional peaks due to the presence of unreacted bipyridine boronic ester (the peaks of the impurities are circled in red in Figure 2.20). Despite this, the characteristic signals are present, confirming the success of the reaction.

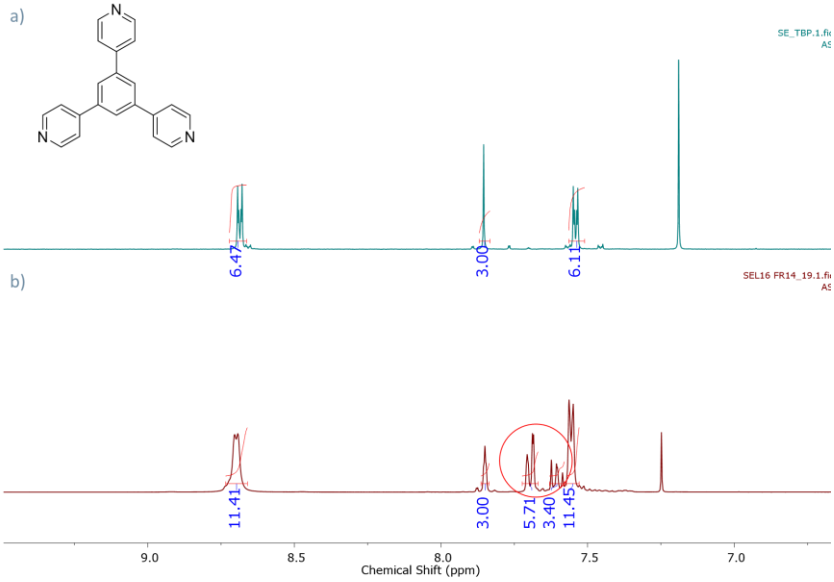

Figure 2.20: a) 1H NMR spectrum of commercial TPB;
b) 1H NMR spectrum of compound (**2**)

Being sure that the reaction would go to completion, the focus shifted to the formation of substituted TPB. To this end, the number of equivalents of the pyridine boronic ester was lowered in order to functionalize only two of three possible positions of the starting 1,3,5-tribromobenzene to obtain 4,4'-(5-bromo-1,3-phenylene)dipyridine (compound **5**) (Figure 2.21).

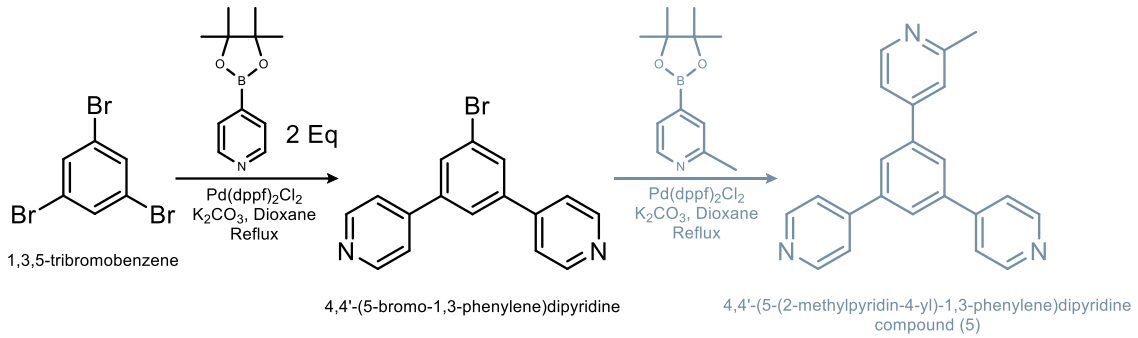

Figure 2.21: First assumed route for the synthesis of compound (**5**)

Unfortunately, the stoichiometric control of the substitutions resulted to be inefficient, preventing the isolation of the disubstituted product. Indeed, only the starting 1,3,5-tribromobenzene and TPB were detected as reaction products.

To overcome this problem, the access to the desired disubstituted molecule had to be found through an alternative synthetic pathway (Figure 2.22).

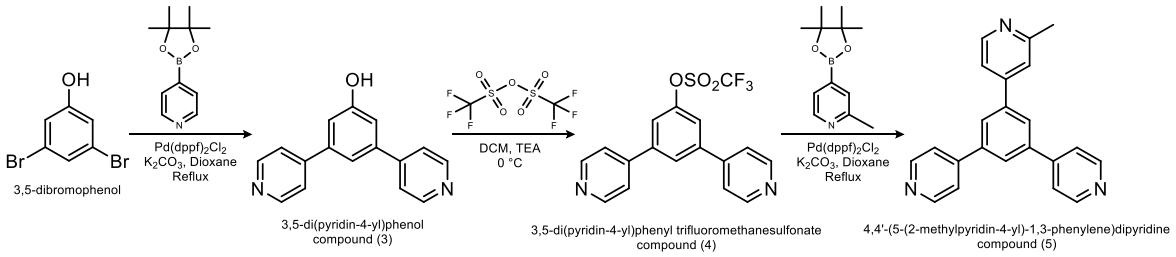

Figure 2.22: Second route for the synthesis of compound (**5**)

Starting from 3,5-dibromophenol, with the cross-coupling, two pyridines are connected to the benzene while the hydroxyl group, under these conditions, is not reactive. Looking at the NMR spectrum, we see 2 singlets belonging to the central benzene part (one singlet integrating 1 and the other integrating 2) and 2 doublets belonging to the hydrogens on the pyridines (both the doublets integrating 4 due to

symmetry). The ^{1}H NMR spectrum of the raw product (compound (**3**)), non-purified, confirms that the reaction was successful (Figure 2.23).

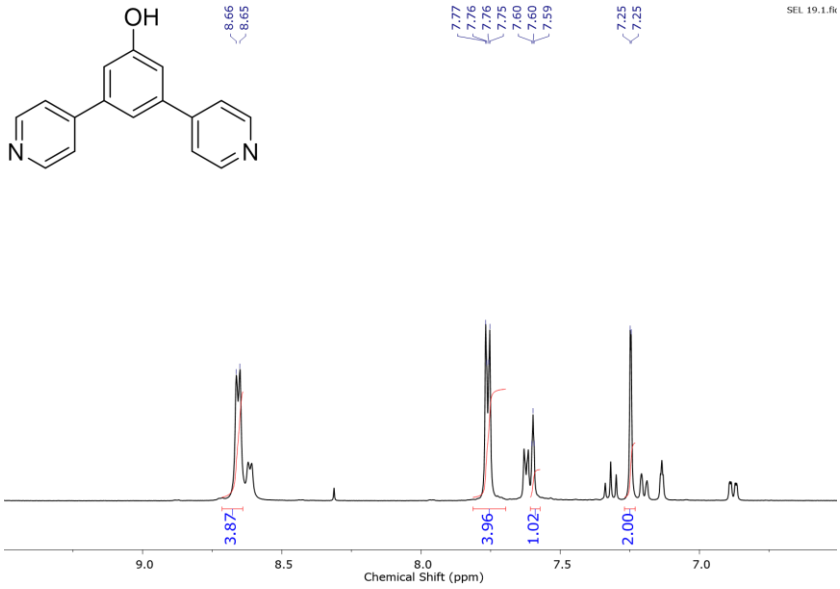

Figure 2.23: ^{1}H NMR spectrum of compound (**3**)

Then, by reaction with triflic anhydride, the hydroxyl group can be activated with a triflate group able to take part in the cross-coupling reaction. The structure of the product is confirmed from NMR. The number of hydrogens of this molecule is the same as the starting 3,5-di(pyridin-4-yl)phenol. The electronegativity of the substituent group influences the shift to downfields of the hydrogen peaks on benzene relative to the pyridine hydrogen peaks. The triflate group is a strong electron-attracting group that attracts to itself the oxygen odd electronic doublets which, by contrast, in phenol are able to participate in the resonance of the benzene ring. The central benzene hydrogens have, in the triflate product, an electron-attracting group close to them which displaces the two singlets between the pyridine hydrogens with respect to the NMR spectrum of the starting molecule. Again, the ^{1}H NMR spectrum confirms the presence of compound (**4**) (Figure 2.24).

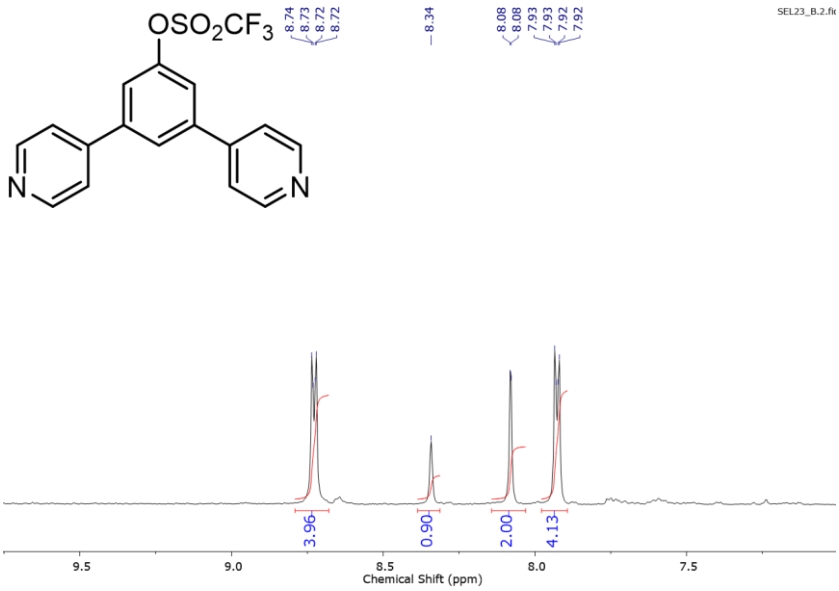

Figure 2.24: ^{1}H NMR spectrum of compound (**4**)

Now the cross-coupling can be performed with a substituted pyridine, and 2-methylpyridine was chosen as test, obtaining 4,4'-(5-(2-methylpyridin-4-yl)-1,3-phenylene)dipyridine (compound (**5**)). In the NMR, the hydrogens belonging to the methyl group can be seen at around 2.6 ppm (Figure 2.25). In addition, the product was confirmed by MS-ESI: calculated 323.4 g/mol $[M+H]^{+}$, found: 324.3 g/mol. The product was collected and recrystallized in chloroform, ready to be used for the catenane synthesis.

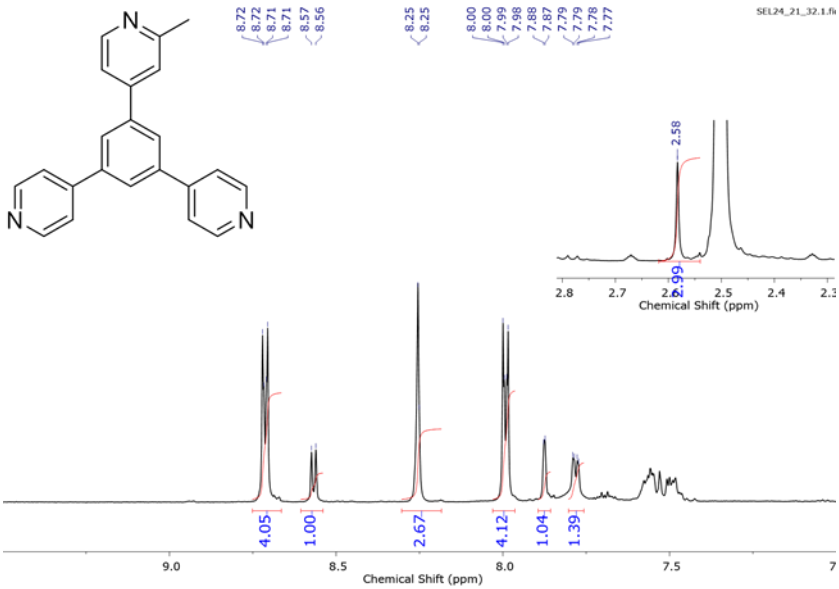

Figure 2.25: ^{1}H NMR spectrum of compound (**5**)

For its potential synthetic simplicity, the synthesis of 1,3,5-tris(2,6-dichloropyridin-4-yl)benzene (compound (**6**))was tried, changing significantly the ligand features. This was done by just performing the cross-coupling directly on the 1,3,5-tribromobenzene (Figure 2.26).

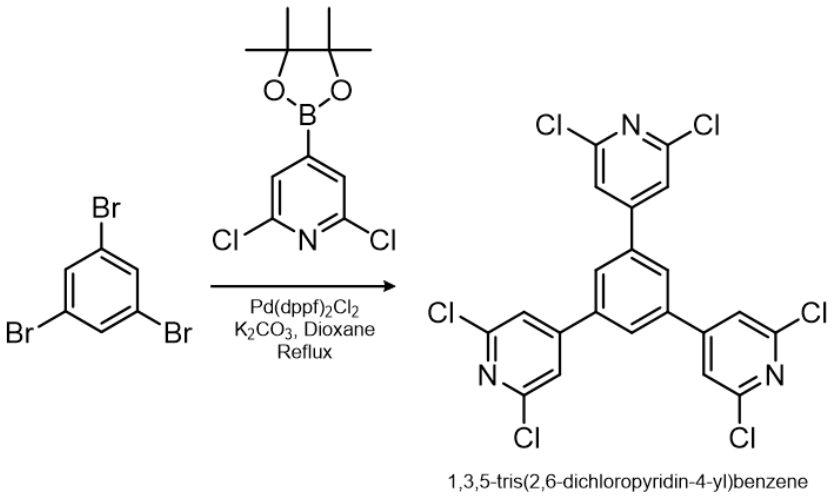

Figure 2.26: Synthesis of 1,3,5-tri(pyridin-4-yl)benzene (**6**)

It is worth noting that while the 2,6-dichloro ligand is perfectly symmetric favoring the stabilization of the final architecture of the catenane, the 2-methyl ligand could have some problems with isomers and enhance of torsional angle. The product reaction was carried out without proceeding to purification.

Having successfully synthesized these compounds, they will in the future be used to test the synthesis of poly-[*n*]-catenanes or other metal-organic structures.

3 Materials and methods

Starting materials and solvents were purchased from commercial suppliers (Alfa Aesar, Apollo Scientific, Fluka, FluoroChem, Honeywell, Sigma Aldrich, TCI, iChemicals) and used without further purification, if not mentioned otherwise.

3.1 Analytical Instrumentation

All the experiments were carried out using the following instrumentation.

Powder X-Ray Diffraction

Bruker D2-Phaser diffractometer equipped with Cu radiation (λ = 1.54184 Å) using Bragg Brentano geometry. The experiments were performed at room temperature.

NMR

Bruker ARS (400 MHz) spectrometer selecting an appropriate number of scans and relaxation time using several deuterium solvents depending on the compound to be analyzed.

High-Resolution Solid-State NMR

BRUKER NEO spectrometer equipped with a commercial 4 mm MAS iProbe. The magnetic field strength was 11.74 T with a spinning speed of 12 kHz. The operative temperature was 298 K with 3600-4800 scans for an appropriate signal-to-noise ratio.

FT-IR

ATR (Attenuated Total Reflection) method using a Varian 640-IR spectrometer by Agilent Technologies equipped with a PIKE MIRacle single reflection ATR by PIKE Technologies. Spectra were taken in the wavelength range of 450 cm^{-1} to 4500 cm^{-1} with 128 scans.

GC-MS

Agilent HP-6890 chromatograph provided with a 5973-mass detector and an Agilent HP-5MS column.

TGA

Thermo-Gravimetrical analyses were determined with a Perkin Elmer Thermal Analysis instrument by the Laboratorio Analisi Chimiche at the Department of Chemistry, Materials and Chemical Engineering (Politecnico di Milano). The temperature ranged from 30 °C to 700 °C with a heating rate of 10 °C/min under nitrogen.

Elemental Analysis

The elemental analysis experiments were performed by the Laboratorio Analisi Chimiche at the Department of Chemistry, Materials and Chemical Engineering, (Politecnico di Milano) using a Costech ECS mod. 4010.

3.2 General Procedures

3.2.1 Catenanes Synthesis

Slow crystallization Three Layer Synthesis

In a 25 mL round-bottomed flask, 30 mg of TPB were suspended in 8 mL of nitrobenzene (if another solvent was used, it is mentioned with the respective quantity). Then, 2 mL of MeOH were added and the mixture was stirred at room temperature until a clear homogeneous solution was obtained. Meanwhile, a given amount of metal salt ($ZnBr_2$ = 32.76 mg, $ZnCl_2$ = 19.83 mg, ZnI_2 = 46.43 mg) was dissolved in 1 mL of MeOH in a glass vial. The ligand solution is transferred to a test tube and 3 mL of methanol were carefully added in order to allow the stratification of the solvents. Then, the metal solution was carefully added to create the third layer, and the test tube was sealed with parafilm to avoid solvent evaporation. Catenanes formed in about 1 week as yellowish transparent crystals.

Computing the metal salt amount:

The general formula of catenanes is $M_{12}L_8$ thus the ratio ligand to metal is 1:1.5

30mg TPB (MW = 309.364 g/mol) = 0.097 mmol * 1.5 = 0.1455 mmol

$ZnBr_2$ (MW = 225.2 g/mol) = 32.767 mg

$ZnCl_2$ (MW = 136.3 g/mol) = 19.829 mg

ZnI_2 (MW = 319.2 g/mol) = 46.444 mg

Fast Crystallization

In a 25 mL round-bottomed flask, 30 mg of TPB were suspended in 8 mL of nitrobenzene (if another solvent was used, it is mentioned with the respective quantity). Then, 2 mL of MeOH were added and the mixture was stirred at room temperature until a clear homogeneous solution was obtained. Meanwhile, a given amount of metal salt ($ZnBr_2$ = 32.76 mg, $ZnCl_2$ = 19.83 mg, ZnI_2 = 46.43 mg) was dissolved in 1mL of MeOH in a glass vial. The metal solution was quickly poured into the ligand solution under vigorous stirring. After the addition of the metal salt, a white precipitate immediately formed giving a suspension which was left stirring for 15 minutes. The formed solid was filtered and left to equilibrate with the atmosphere to eliminate any solvent attached to the surface of the microcrystals.

Mechanochemical Grinding Synthesis

30 mg of TPB and a given amount of metal salt ($ZnBr_2$ = 32.76 mg, $ZnCl_2$ = 19.83 mg, ZnI_2 = 46.43 mg) were grinded in a mortar for at least 15 minutes to obtain a white powder.

3.2.2 Adsorption Experiments

30 mg of the poly-[*n*]-catenane were added in a round-bottom flask with 5mL of the guest material. The system was stirred for a given amount of time typically overnight. Then, the stirring was stopped, and the solution was allowed to settle. The mixture was filtered, and the resulting off-white solid was dried in open air prior to the analysis.

3.2.3 Isomers Separation Experiments

Flask Experiment

30 mg of the poly-[*n*]-catenane were added in a round-bottom flask. A mixture of two or three different isomers was prepared and added to the flask. The system was stirred for a given time, typically overnight. Then, the stirring was stopped, and the solution was allowed to settle. The mixture was filtered, and the resulting off-white solid was dried in open air prior to the analysis.

Column-like Experiment

A small piece of cotton was pushed on the bottom of a Pasteur pipette to avoid any solid leakage. 200 mg of the poly-[*n*]-catenane sample (amorphous or crystalline depending on the experiment) were packed in the pipette. The rest of the pipette was filled with a solution of the isomers. The system was left at rest, waiting for all the liquid to percolate down the pipette through the solid and collected in a vial below. When all the liquid passed through, the solid was dried in open air and both parts analyzed.

3.2.4 Ligand Synthesis

*Synthesis of 4-pyridineboronic acid pinacol ester (**1**)*

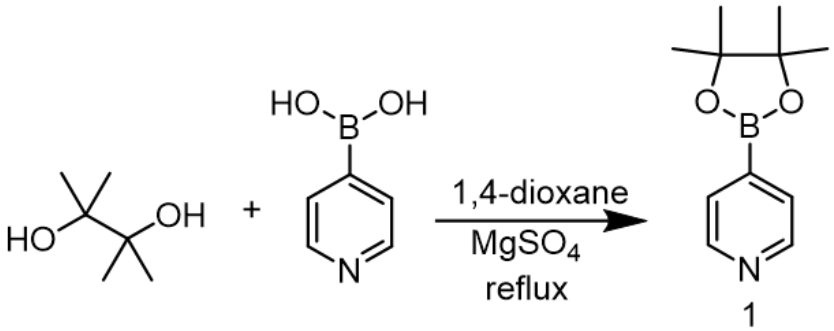

1

Briefly, in a 250 mL round-bottomed flask, 4-pyridineboronic acid (3 g, 24.41 mmol), 2,3-dimethyl-2,3-butanediol (3.17 g, 26.85 mmol) and magnesium sulfate (6.46 g, 53.7 mmol) were dissolved in 1,4-dioxane (122 mL). The mix was heated to reflux for 24 h. the reaction was then cooled to room temperature. The solution was

condensed under vacuum and the residue was dried over high vacuum to give a white solid that was used without further purification.

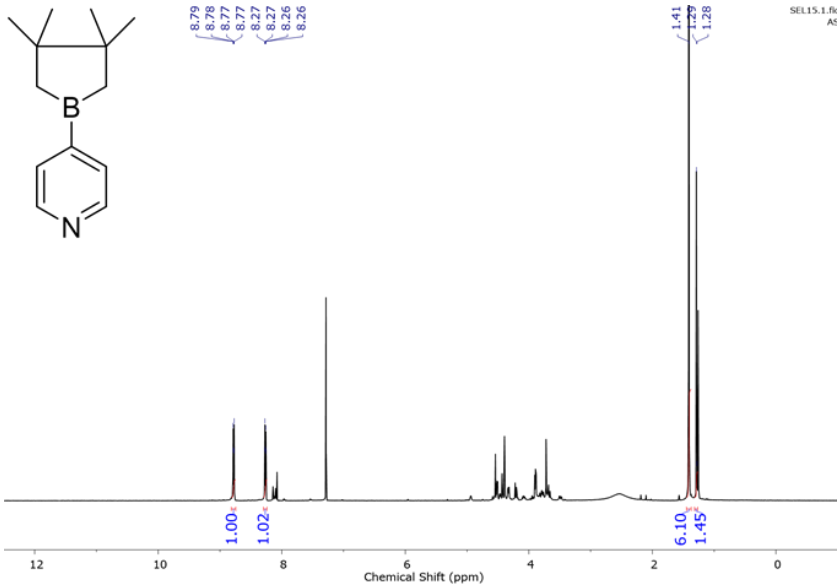

Figure 3.1: ^{1}H NMR spectrum of compound (**1**)

Synthesis of 1,3,5-tri(pyridin-4-yl)benzene (2)

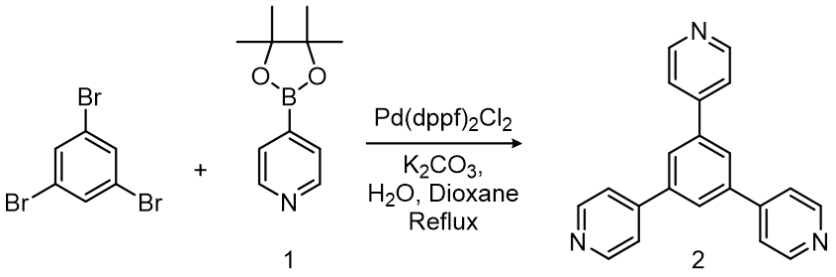

In a 500 mL two-necked round-bottom flask dioxane (153.6 mL) and a solution of K_2CO_3 (11.24 g, 81.4 mmol) in H_2O (40.7 mL) were added and degassed for 10 minutes. Then 1,3,5-tribromobenzene (2.56 g, 8.14 mmol), 4-pyridineboronic acid pinacol ester (1) (5 g, 24.41 mmol, 3Eq), tricyclohexylphosphine (684 mg, 2.44 mmol) and [1,1'-bis(diphenyl-phospino)ferrocene]palladium(II) chloride (893 mg, 1.22 mmol, 15 mol%) were added. The mixture was degassed under stirring for further 10 minutes and then refluxed under nitrogen atmosphere for 48 h. The completion of the reaction was checked by TLC (dichloromethane in ammonia atmosphere, R_f: 0.283) then the mixture was cooled to room temperature and 100 mL of dichloromethane were added. The organic phase was separated and washed with

H_2O (2x40 mL), dried over Na_2SO_4, and the solvent was removed under reduced pressure to yield a dark brown oil. The crude was purified by flash column chromatography on silica (DCM:TEA=97:3) to yield 1,3,5-tri(pyridin-4-yl)benzene as a white solid. The characterization of the product was in line with that reported in literature.

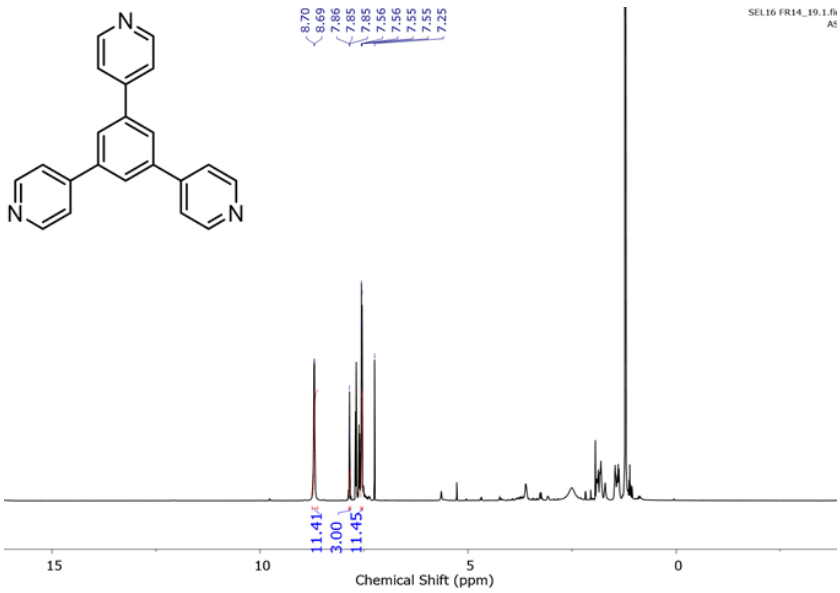

Figure 3.2: ^{1}H NMR spectrum of compound (**2**)

*Synthesis of 3,5-di(pyridin-4-yl)phenol (**3**)*

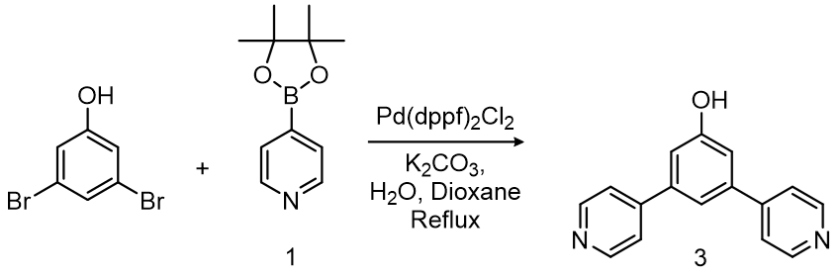

In a 500 mL two-necked round-bottom flask dioxane (149.8 mL) and a solution of K_2CO_3 (10.97 g, 79.39 mmol) in H_2O (39.7 mL) were added and degassed for 10 minutes. Then 3,5-dibromophenol (2 g, 7.94 mmol), 4-pyridineboronic acid pinacol ester (1) (3.91 g, 19.05 mmol, 2.4Eq), tricyclohexylphosphine (668 mg, 2.38 mmol) and [1,1'-bis(diphenyl-phospino)ferrocene]palladium(II) chloride (973 mg, 1.19 mmol, 15 mol%) were added. The mixture was degassed under stirring for further 10 minutes and then refluxed under nitrogen atmosphere for 48 h. The completion

of the reaction was checked by TLC (chloroform, R_f= 0.333) then the solvents were evaporated from the reaction mixture, and the rest were transferred into a flask with chloroform and water. HCl (12 M) is added until the aqueous layer reaches pH=0 and the precipitate dissolves completely. The mix is extracted and washed with 3x150 mL of chloroform and the organic layer is discarded. The aqueous layer is transferred in a beaker with a stirrer bar and $KHCO_3$ (sat.) solution is added until pH=7. A large amount of white solid is formed and filtered. The solid was suspended in cool ethanol and filtered to remove the impurities. The product is dried and collected as a solid (1.435 g, yield: 72.8%).

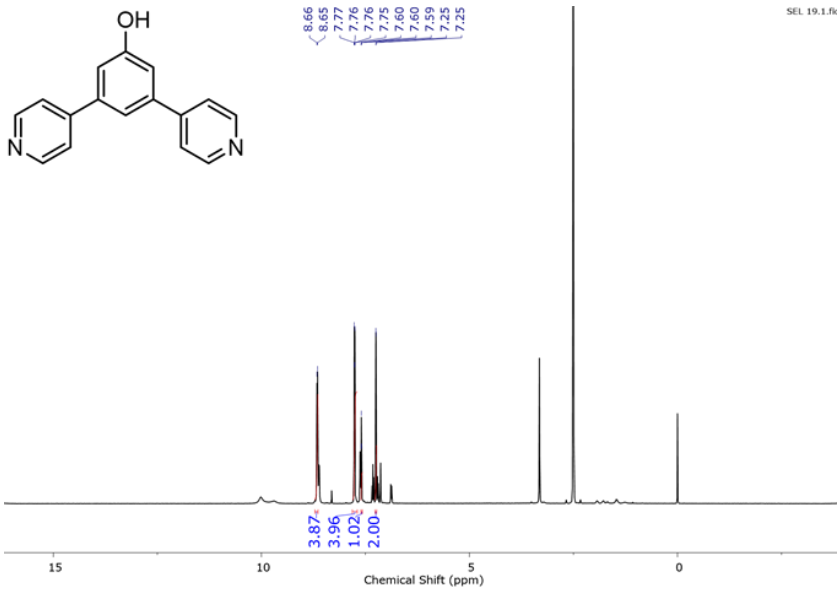

Figure 3.3: ^{1}H NMR spectrum of compound (**3**)

*Synthesis of 3,5-di(pyridin-4-yl) phenyltrifluoromethanesulfonate (**4**)*

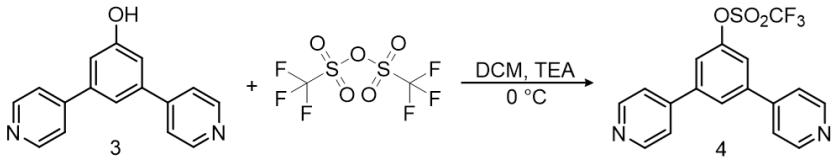

In a 250 mL round-bottomed flask, 3,5-dibromophenol (3) (2.2 g, 8.86 mmol) was dissolved in DCM (88.6 mL) and cooled to 0 °C. NEt3 (1.5 mL, 10.63 mmol, 1.2equiv) was added dropwise to the solution, which was followed by the addition of triflic anhydride (1.8 mL, 10.63 mmol, 1.2 equivalents). After 5 minutes, the ice bath was removed, and the reaction was monitored by TLC (DCM:MeOH=95:5, R_f=0.6). Once

the phenol was completely consumed, the reaction was stopped. The solvent was evaporated under vacuum and the residue was purified by flash column chromatography (DCM:MeOH=98:2) to get the desired aryl triflate.

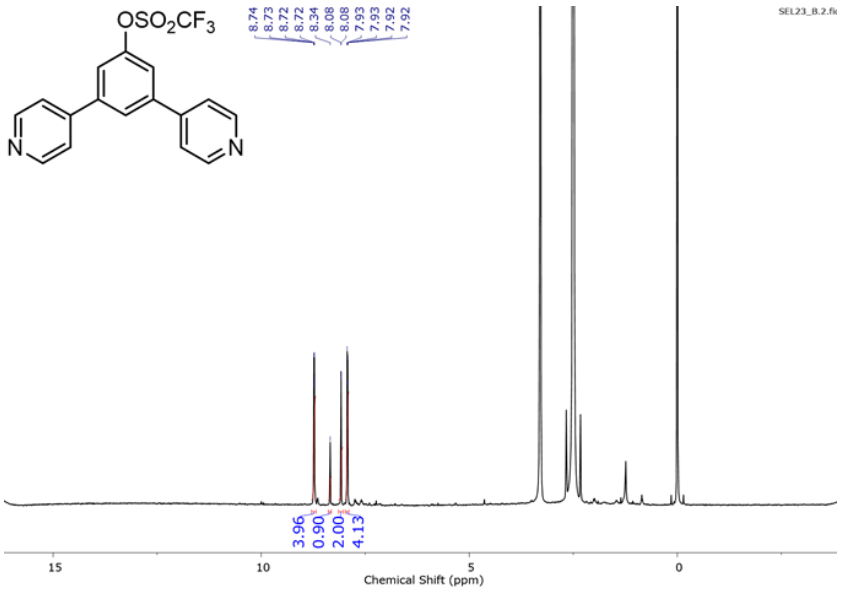

Figure 3.4: ^{1}H NMR spectrum of compound (**4**)

*Synthesis of 4,4'-(5-(2-methylpyridin-4-yl)-1,3-phenylene) dipyridine (**5**)*

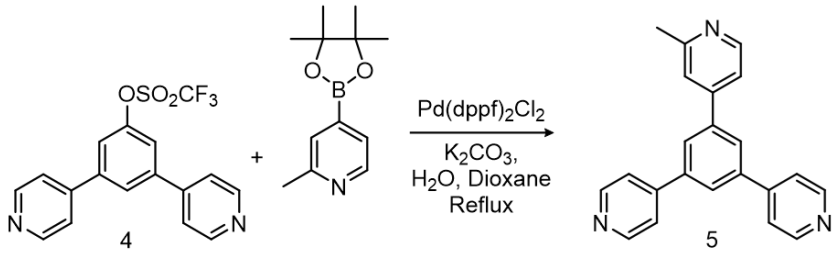

In a 50 mL two-necked round-bottom flask dioxane (14.87 mL) and a solution of K_2CO_3 (1.09 g, 7.88 mmol) in H_2O (3.94 mL) were added and degassed for 10 minutes. Then 3,5-di(pyridin-4-yl)phenyl trifluoromethanesulfonate (4) (300 mg, 0.789 mmol), 2-methyl-4-pyridineboronic acid pinacol ester (345.6 mg, 1.577 mmol, 2Eq), tricyclohexylphosphine (66.3 mg, 0.236 mmol) and [1,1'-bis(diphenyl-phospino)ferrocene]palladium(II) chloride (96.59 mg, 0.118 mmol, 15 mol%) were added. The mixture was degassed under stirring for further 10 minutes, and then refluxed under nitrogen atmosphere for 48 h. The completion of the reaction was

checked by TLC (dichloromethane in ammonia atmosphere, R_f= 0.91) then the mixture was cooled to room temperature and 100 mL of dichloromethane were added. The organic phase was separated and washed with H_2O (2x40 mL), dried over Na_2SO_4, and the solvent was removed under reduced pressure to yield a dark brown oil. The crude was purified by flash column chromatography on silica (DCM:TEA=97:3) to yield 4,4'-(5-(2-methylpyridin-4-yl)-1,3-phenylene)dipyridine (206 mg, yield: 80.8%).

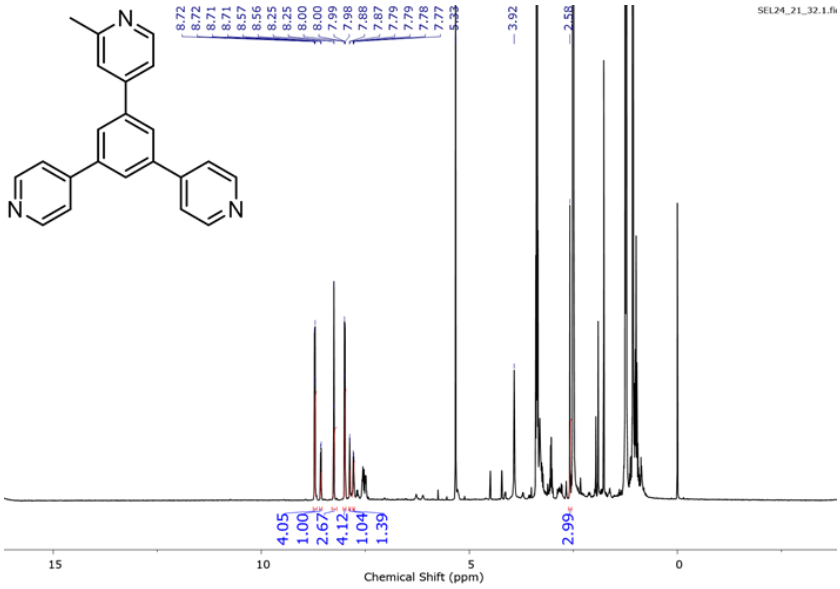

Figure 3.5: ^{1}H NMR spectrum of compound (**5**)

4 Conclusions and further studies

In this thesis I have dealt with the nature of the research I have carried out over the past few months.

First of all, I started experimenting with the possibility of synthesizing an $M_{12}L_8$ poly-[*n*]-catenane, which until now has only been synthesized by instant synthesis. It has been shown that the same structure can be generated without the use of solvents. The poly-[*n*]-catenane formed was found to be in an amorphous phase, contrary to what was reported for the instant synthesis of the same product. In this regard, we tested and confirmed the inclusion of solvents that could play a template effect on the system for a transformation into a crystalline phase. The green approach that guided us to a mechano-chemical synthesis led us to look for a way to recycle this material in an increasingly waste-free way. We were able to recycle the organic ligand by immersion and permanence in water so that it can be reused again and again.

After the synthesis of the amorphous phase, we looked for possible uses. We first tried our hand at storage, trying to include different molecules due to the presence of host-guest interactions. We then confirmed that molecules with aromatic rings, once they have helped their way into the cages, are able to do an excellent job of keeping the structure crystalline over time. For a better understanding of the structure, we also tried to change the counterion of the Secondary Building Unit, discovering a connection with the crystallinity of the system. In addition, we did experiments to test the interaction of interlocked cages with different isomers for possible application in the field of separation and isomer recognition. We started with the three structural isomers of dichlorobenzene, began to see their synergy with catenane, and will continue to work in this direction.

While working on the aspects described above, organic chemistry was also used to synthesize new ligands. Initially by synthesizing the primary TPB ligand, we then tried docking substituents with different characteristics.

Given the large number of research paths that have opened up in this work, it is essential to devote oneself to future work. The treated material, belonging to the category of catenanes, should share all its characteristic properties. So, in the future gas adsorption, drug delivery and catalysis tests would be carried out. Obviously, we will continue to work on the field of isomer recognition, trying with new molecules, perhaps even enantiomers, trying to design possible chromatographic columns. In addition to the already obtained ligands, new TPB derivatives with various functional groups will be synthesized and used instead of TPB, following the same crystallization conditions described in this thesis. It is known that small changes in the self-assembling building blocks can give rise to completely diverse structures. Using various TPB derivatives the role of the aromatic-aromatic interactions in the formation of the poly-[n]-catenanes will be investigated.

Bibliography

[1] S. R. Batten, N. R. Champness, X. M. Chen, J. Garcia-Martinez, S. Kitagawa, L. Öhrström, M. O'Keeffe, M. P. Suh and J. Reedijk, "Terminology of metal-organic frameworks and coordination polymers (IUPAC recommendations 2013)," *Pure and Applied Chemistry,* vol. 85, no. 8, 2013.

[2] M. Safaei, M. M. Foroughi, N. Ebrahimpoor, S. Jahani, A. Omidi and M. Khatami, "A review on metal-organic frameworks: Synthesis and applications," *TrAC - Trends in Analytical Chemistry,* vol. 118, 2019.

[3] J. L. Rowsell and O. M. Yaghi, "Metal-organic frameworks: A new class of porous materials," *Microporous and Mesoporous Materials,* vol. 73, no. 1-2, pp. 3-14, 8 2004.

[4] P. Z. Moghadam, A. Li, S. B. Wiggin, A. Tao, A. G. Maloney, P. A. Wood, S. C. Ward and D. Fairen-Jimenez, "Development of a Cambridge Structural Database Subset: A Collection of Metal-Organic Frameworks for Past, Present, and Future," *Chemistry of Materials,* vol. 29, no. 7, 2017.

[5] N. Stock and S. Biswas, "Synthesis of Metal-Organic Frameworks (MOFs): Routes to Various MOF Topologies, Morphologies, and Composites," *Chemical Reviews,* vol. 112, no. 2, pp. 933-969, 2 2012.

[6] X. Zhang, Z. Chen, X. Liu, S. L. Hanna, X. Wang, R. Taheri-Ledari, A. Maleki, P. Li and O. K. Farha, "A historical overview of the activation and porosity of metal-organic frameworks," *Chemical Society Reviews,* vol. 49, no. 20, 2020.

[7] S. R. V. Moises A Carreon, "Metal-Organic Frameworks History and Structural Features," 2020.

[8] O. K. Farha, I. Eryazici, N. C. Jeong, B. G. Hauser, C. E. Wilmer, A. A. Sarjeant, R. Q. Snurr, S. T. Nguyen, A. Ö. Yazaydin and J. T. Hupp, "Metal-organic framework materials with ultrahigh surface areas: Is the sky the limit?," *Journal of the American Chemical Society,* vol. 134, no. 36, pp. 15016-15021, 9 2012.

[9] H. Li, K. Wang, Y. Sun, C. T. Lollar, J. Li and H. C. Zhou, "Recent advances in gas storage and separation using metal–organic frameworks," *Materials Today,* vol. 21, no. 2, pp. 108-121, 3 2018.

[10] Y. Ma, W. Tong, H. Zhou and S. L. Suib, "A review of zeolite-like porous materials," *Microporous and Mesoporous Materials,* vol. 37, no. 1-2, pp. 243-252, 5 2000.

[11] J. C. B. Jr., "Coordination Polymers," *Prep. Inorg. React.,* vol. 1, 1964.

[12] B. F. Hoskins and R. Robson, "Infinite polymeric frameworks consisting of three dimensionally linked rod-like segments," *Journal of the American Chemical Society,* vol. 111, no. 15, pp. 5962-5964, 7 1989.

[13] R. R. B. F. Hoskins, "Design and construction of a new class of scaffolding-like materials comprising infinite polymeric frameworks of 3D-linked molecular rods. A reappraisal of the zinc cyanide and cadmium cyanide structures and the synthesis and structure of the diamond-rela," *J. Am. Chem. Soc.,* pp. 1546-1554, 1990.

[14] O. M. Yaghi and H. Li, "Hydrothermal Synthesis of a Metal-Organic Framework Containing Large Rectangular Channels," *Journal of the American Chemical Society,* vol. 117, no. 41, 1995.

[15] O. M. Yaghi, G. Li and H. Li, "Selective binding and removal of guests in a microporous metal–organic framework," *Nature,* vol. 378, no. 6558, 1995.

[16] S. Khan, F. Vakil, M. Zeeshan and M. Shahid, "Postsynthetic Modification (PSM) in Metal-Organic Frameworks (MOFs): Icing on the Cake," *ACS Symposium Series,* vol. 1393, 2021.

[17] U. Mueller, M. Schubert, F. Teich, H. Puetter, K. Schierle-Arndt and J. Pastré, "Metal-organic frameworks - Prospective industrial applications," *Journal of Materials Chemistry,* vol. 16, no. 7, pp. 626-636, 2006.

[18] A. Kirchon, L. Feng, H. F. Drake, E. A. Joseph and H. C. Zhou, "From fundamentals to applications: a toolbox for robust and multifunctional MOF materials," *Chemical Society Reviews,* vol. 47, no. 23, pp. 8611-8638, 12 2018.

[19] D. Farrusseng, Metal-Organic Frameworks: Applications from Catalysis to Gas Storage, 2011.

[20] L. Jiao, Y. Wang, H. L. Jiang and Q. Xu, "Metal–Organic Frameworks as Platforms for Catalytic Applications," *Advanced Materials,* vol. 30, no. 37, 2018.

[21] A. Dhakshinamoorthy, M. Opanasenko, J. Čejka and H. Garcia, "Metal organic frameworks as heterogeneous catalysts for the production of fine chemicals," *Catalysis Science and Technology,* vol. 3, no. 10, pp. 2509-2540, 10 2013.

[22] M. Fujita, S. Washizu, K. Ogura and Y. J. Kwon, "Preparation, Clathration Ability, and Catalysis of a Two-Dimensional Square Network Material Composed of Cadmium(II) and 4,4'-Bipyridine," *Journal of the American Chemical Society,* vol. 116, no. 3, 1994.

[23] J. Yang and Y. W. Yang, "Metal–Organic Frameworks for Biomedical Applications," *Small,* vol. 16, no. 10, 3 2020.

[24] Y. Sun, L. Zheng, Y. Yang, X. Qian, T. Fu, X. Li, Z. Yang, H. Yan, C. Cui and W. Tan, "Metal–Organic Framework Nanocarriers for Drug Delivery in Biomedical Applications," *Nano-Micro Letters,* vol. 12, no. 1, p. 103, 12 2020.

[25] P. Kumar, A. Deep and K. H. Kim, "Metal organic frameworks for sensing applications," *TrAC - Trends in Analytical Chemistry,* vol. 73, 2015.

[26] M. Yoshizawa, J. K. Klosterman and M. Fujita, "Functional molecular flasks: new properties and reactions within discrete, self-assembled hosts," *Angewandte Chemie - International Edition,* vol. 48, no. 19, pp. 3418-3438, 4 2009.

[27] H. W. Langmi, J. Ren, B. North, M. Mathe and D. Bessarabov, "Hydrogen storage in metal-organic frameworks: A review," *Electrochimica Acta,* vol. 128, 2014.

[28] M. T. Kapelewski, T. Runčevski, J. D. Tarver, H. Z. Jiang, K. E. Hurst, P. A. Parilla, A. Ayala, T. Gennett, S. A. Fitzgerald, C. M. Brown and J. R. Long, "Record High Hydrogen Storage Capacity in the Metal-Organic Framework Ni_2(*m*-dobdc) at Near-Ambient Temperatures," *Chemistry of Materials,* vol. 30, no. 22, 2018.

[29] H. Kim and C. S. Hong, "MOF-74-type frameworks: tunable pore environment and functionality through metal and ligand modification," *CrystEngComm,* vol. 23, no. 6, 2021.

[30] G. Parks, R. Boyd, J. Cornish and R. Remick, "Hydrogen Station Compression, Storage, and Dispensing Technical Status and Costs: Systems Integration," 2014.

[31] Y. He, F. Chen, B. Li, G. Qian, W. Zhou and B. Chen, "Porous metal–organic frameworks for fuel storage," *Coordination Chemistry Reviews,* vol. 373, 2018.

[32] W. Xu and O. M. Yaghi, "Metal-Organic Frameworks for Water Harvesting from Air, Anywhere, Anytime," *ACS Central Science,* vol. 6, no. 8, 2020.

[33] N. Hanikel, M. S. Prévot and O. M. Yaghi, "MOF water harvesters," *Nature Nanotechnology,* vol. 15, no. 5, pp. 348-355, 5 2020.

[34] Z.-Y. Gu, C.-X. Yang, N. Chang and X.-P. Yan, "Metal–Organic Frameworks for Analytical Chemistry: From Sample Collection to Chromatographic Separation," *Accounts of Chemical Research,* vol. 45, no. 5, pp. 734-745, 5 2012.

[35] W. Q. Tang, J. Y. Xu and Z. Y. Gu, "Metal–Organic-Framework-based Gas Chromatographic Separation," *Chemistry - An Asian Journal,* vol. 14, no. 20, 2019.

[36] X. Zhao, Y. Wang, D. S. Li, X. Bu and P. Feng, "Metal–Organic Frameworks for Separation," *Advanced Materials,* vol. 30, no. 37, 9 2018.

[37] H. Jiang, K. Yang, X. Zhao, W. Zhang, Y. Liu, J. Jiang and Y. Cui, "Highly Stable Zr(IV)-Based Metal-Organic Frameworks for Chiral Separation in Reversed-Phase Liquid Chromatography," *Journal of the American Chemical Society,* vol. 143, no. 1, 2021.

[38] M. N. Corella-Ochoa, J. B. Tapia, H. N. Rubin, V. Lillo, J. González-Cobos, J. L. Núñez-Rico, S. R. Balestra, N. Almora-Barrios, M. Lledós, A. Guëll-Bara, J. Cabezas-Giménez, E. C. Escudero-Adán, A. Vidal-Ferran, S. Calero, M. Reynolds, C. Martí-Gastaldo and J. R. Galán-Mascarós, "Homochiral Metal-Organic Frameworks for Enantioselective Separations in Liquid Chromatography," *Journal of the American Chemical Society,* vol. 141, no. 36, 2019.

[39] V. Gold, Ed., The IUPAC Compendium of Chemical Terminology, Research Triangle Park, NC: International Union of Pure and Applied Chemistry (IUPAC), 2019.

[40] G. Gil-Ramírez, D. A. Leigh, A. J. Stephens and D. A. Leigh, "Catenanes: Fifty Years of Molecular Links Angewandte Reviews".

[41] H. Frisch, I. Martin and H. Mark, "Zur Struktur der Polysiloxene. I," *Monatshefte fur Chemie,* vol. 84, no. 2, pp. 250-256, 1953.

[42] F. Patat and P. Derst, "Über den thermischen Abbau des polymeren Phosphornitrilchlorids," *Angewandte Chemie,* vol. 71, no. 3, pp. 105-110, 2 1959.

[43] C. D. Wu and M. Zhao, "Incorporation of Molecular Catalysts in Metal–Organic Frameworks for Highly Efficient Heterogeneous Catalysis," *Advanced Materials,* vol. 29, no. 14, 2017.

[44] H. W. Gibson, M. C. Bheda and P. T. Engen, "Rotaxanes, catenanes, polyrotaxanes, polycatenanes and related materials," *Progress in Polymer Science,* vol. 19, no. 5, pp. 843-945, 1 1994.

[45] Z. Niu and H. W. Gibson, "Polycatenanes," *Chemical Reviews,* vol. 109, no. 11, 2009.

[46] H. Lei, J. Zhang, L. Wang and G. Zhang, "Dimensional and shape properties of a single linear polycatenane: Effect of catenation topology," *Polymer,* vol. 212, p. 123160, 1 2021.

[47] F. M. Raymo and J. F. Stoddart, "Interlocked Macromolecules," *Chemical Reviews,* vol. 99, no. 7, 1999.

[48] Z. Li, W. Liu, J. Wu, S. H. Liu and J. Yin, "Synthesis of [2]catenanes by template-directed clipping approach," *Journal of Organic Chemistry,* vol. 77, no. 16, 2012.

[49] W. R. Dichtel, O. Š. Miljanić, W. Zhang, J. M. Spruell, K. Patel, I. Aprahamian, J. R. Heath and J. F. Stoddart, "Kinetic and Thermodynamic Approaches for the Efficient Formation of Mechanical Bonds," *Accounts of Chemical Research,* vol. 41, no. 12, pp. 1750-1761, 12 2008.

[50] J. F. Stoddart, M. A. Olson, L. Fang, A. Coskun and A. N. Basuray, "Polycatenation under kinetic and thermodynamic control.," *Polymer Preprints (American Chemical Society, Division of Polymer Chemistry),* vol. 51, no. 2, 2010.

[51] D. B. Amabilino, P. R. Ashton, V. Balzani, S. E. Boyd, A. Credi, J. Y. Lee, S. Menzer, J. F. Stoddart, M. Venturi and D. J. Williams, "Oligocatenanes Made to Order," *Journal of the American Chemical Society,* vol. 120, no. 18, pp. 4295-4307, 5 1998.

[52] D. B. Amabilino, P. R. Ashton, A. S. Reder, N. Spencer and J. F. Stoddart, "Olympiadane," *Angewandte Chemie International Edition in English,* vol. 33, no. 12, pp. 1286-1290, 6 1994.

[53] P. R. Ashton, C. L. Brown, E. J. T. Chrystal, K. P. Parry, M. Pietraszkiewicz, N. Spencer and J. F. Stoddart, "Molecular Trains: The Self-Assembly and Dynamic Properties of Two New Catenaries," *Angewandte Chemie International Edition in English,* vol. 30, no. 8, pp. 1042-1045, 8 1991.

[54] T. Takata, N. Kihara and Y. Furusho, "Polyrotaxanes and polycatenanes: Recent advances in syntheses and applications of polymers comprising of interlocked structures," *Advances in Polymer Science,* vol. 171, 2004.

[55] D. Sluysmans and J. F. Stoddart, "The Burgeoning of Mechanically Interlocked Molecules in Chemistry," *Trends in Chemistry,* vol. 1, no. 2, pp. 185-197, 5 2019.

[56] V. Blanco, D. A. Leigh and V. Marcos, "Artificial switchable catalysts," *Chemical Society Reviews,* vol. 44, no. 15, pp. 5341-5370, 2015.

[57] S. F. M. van Dongen, S. Cantekin, J. A. A. W. Elemans, A. E. Rowan and R. J. M. Nolte, "Functional interlocked systems," *Chem. Soc. Rev.,* vol. 43, no. 1, pp. 99-122, 2014.

[58] J. Riebe and J. Niemeyer, "Mechanically Interlocked Molecules for Biomedical Applications," *European Journal of Organic Chemistry,* vol. 2021, no. 37, 2021.

[59] H. Chen and J. Fraser Stoddart, "From molecular to supramolecular electronics," *Nature Reviews Materials,* vol. 6, no. 9, 2021.

[60] M. J. Langton and P. D. Beer, "Rotaxane and Catenane Host Structures for Sensing Charged Guest Species," *Accounts of Chemical Research,* vol. 47, no. 7, pp. 1935-1949, 7 2014.

[61] A. Caballero, F. Zapata and P. D. Beer, "Interlocked host molecules for anion recognition and sensing," *Coordination Chemistry Reviews,* vol. 257, no. 17-18, pp. 2434-2455, 9 2013.

[62] N. H. Evans and P. D. Beer, "Progress in the synthesis and exploitation of catenanes since the Millennium," *Chemical Society Reviews,* vol. 43, no. 13, 2014.

[63] I. Aprahamian, "The Future of Molecular Machines," *ACS Central Science,* vol. 6, no. 3, pp. 347-358, 3 2020.

[64] J. Heine, J. Schmedt Auf Der Günne and S. Dehnen, "Formation of a strandlike polycatenane of icosahedral cages for reversible one-dimensional encapsulation of guests," *Journal of the American Chemical Society,* vol. 133, no. 26, 2011.

[65] E. C. Constable, G. Zhang, C. E. Housecroft and J. A. Zampese, "Zinc(ii) coordination polymers, metallohexacycles and metallocapsules - Do we understand self-assembly in metallosupramolecular chemistry: Algorithms or serendipity?," *CrystEngComm,* vol. 13, no. 22, pp. 6864-6870, 11 2011.

[66] K. Biradha and M. Fujita, "A Springlike 3D-Coordination Network That Shrinks or Swells in a Crystal-to-Crystal Manner upon Guest Removal or Readsorption**".

[67] R. R. S. R. Batten, "Interpenetrating Nets: Ordered, Periodic Entanglement," *Angewandte Chemie,* 1998.

[68] S. Torresi, A. Famulari, J. Martí-Rujas and J. Martí-Rujas, "Kinetically Controlled Fast Crystallization of $M_{12}L_8$ Poly-[*n*]-catenanes Using the 2,4,6-Tris(4-pyridyl)benzene Ligand and ZnCl2in an Aromatic Environment," *Journal of the American Chemical Society,* vol. 142, no. 20, 2020.

[69] B. F. H. R. R. S. R. Pattern, "Two Interpenetrating 3D Networks Which Generate Spacious Sealed-Off Compartments Enclosing of the Order of 20 Solvent Molecules in the Structures of $Zn(CN)(NO_3)(tpt)_{2/3}$.cntdot.solv (tpt =

2,4,6-tri(4-pyridyl)-1,3,5-triazine, solv = .apprx.3/4C2H2Cl4.cntdo," *J. Am. Chem. Soc.,* pp. 5385-5386, 1995.

[70] P. T. Anastas and J. C. Warner, "Green Chemistry: Theory and Practice," *Green Chemistry: Theory and Practice, Oxford University Press, New York,* 1998.

[71] S. L. James, C. J. Adams, C. Bolm, D. Braga, P. Collier, T. Friić, F. Grepioni, K. D. Harris, G. Hyett, W. Jones, A. Krebs, J. MacK, L. Maini, A. G. Orpen, I. P. Parkin, W. C. Shearouse, J. W. Steed and D. C. Waddell, "Mechanochemistry: Opportunities for new and cleaner synthesis," *Chemical Society Reviews,* vol. 41, no. 1, 2012.

[72] M. A. P. Martins, C. P. Frizzo, D. N. Moreira, L. Buriol and P. Machado, "Solvent-Free Heterocyclic Synthesis," *Chemical Reviews,* vol. 109, no. 9, pp. 4140-4182, 9 2009.

[73] J. Martí-Rujas, S. Elli, A. Sacchetti and F. Castiglione, "Mechanochemical synthesis of mechanical bonds in $M_{12}L_8$poly-[*n*]-catenanes," *Dalton Transactions,* vol. 51, no. 1, 2022.

[74] G. Kaupp, "Mechanochemistry: The varied applications of mechanical bond-breaking," *CrystEngComm,* vol. 11, no. 3, 2009.

[75] G. W. V. Cave, C. L. Raston and J. L. Scott, "Recent advances in solventless organic reactions: towards benign synthesis with remarkable versatility," *Chemical Communications,* no. 21, pp. 2159-2169, 10 2001.

[76] V. V. Boldyrev and K. Tkáčová, "Mechanochemistry of solids: Past, present, and prospects," *Journal of Materials Synthesis and Processing,* vol. 8, no. 3-4, 2000.

[77] R. Seetharaj, P. V. Vandana, P. Arya and S. Mathew, "Dependence of solvents, pH, molar ratio and temperature in tuning metal organic framework architecture," *Arabian Journal of Chemistry,* vol. 12, no. 3, 2019.

[78] Q.-F. Sun, J. Iwasa, D. Ogawa, Y. Ishido, S. Sato, T. Ozeki, Y. Sei, K. Yamaguchi and M. Fujita, "Self-Assembled M24L48 Polyhedra and Their Sharp Structural

Switch upon Subtle Ligand Variation," *Science,* vol. 328, no. 5982, pp. 1144-1147, 5 2010.

[79] S. Yuan, L. Feng, K. Wang, J. Pang, M. Bosch, C. Lollar, Y. Sun, J. Qin, X. Yang, P. Zhang, Q. Wang, L. Zou, Y. Zhang, L. Zhang, Y. Fang, J. Li and H. C. Zhou, "Stable Metal–Organic Frameworks: Design, Synthesis, and Applications," *Advanced Materials,* vol. 30, no. 37, 2018.

[80] B. Li, Q.-Q. Yan, Z.-Q. Xu, Y.-B. Xu and G.-P. Yong, "Tuning the interpenetration of metal–organic frameworks through changing ligand functionality: effect on gas adsorption properties," *CrystEngComm,* vol. 22, no. 3, pp. 506-514, 2020.

[81] D. Blakemore, "Chapter 1:Suzuki–Miyaura Coupling," *RSC Drug Discovery Series,* Vols. 2016-January, no. 52, pp. 1-69, 5 2016.

[82] Q. Wu, P. M. Rauscher, X. Lang, R. J. Wojtecki, J. J. De Pablo, M. J. Hore and S. J. Rowan, "Poly[*n*]catenanes: Synthesis of molecular interlocked chains," *Science,* vol. 358, no. 6369, 2017.

[83] "BASF Metal Organic Frameworks (MOFs): Innovative Fuel Systems for Natural Gas Vehicles (NGVs)," *Chem. Soc. Rev.,* vol. 43, no. 16, 2014.

[84] S. Fortun, P. Beauclair and A. R. Schmitzer, "Metformin as a versatile ligand for recyclable palladium-catalyzed cross-coupling reactions in neat water," *RSC Advances,* vol. 7, no. 34, pp. 21036-21044, 2017.

[85] A. Zolriasatein, A. Shokuhfar, F. Safari and N. Abdi, "Comparative study of SPEX and planetary milling methods for the fabrication of complex metallic alloy nanoparticles; Comparative study of SPEX and planetary milling methods for the fabrication of complex metallic alloy nanoparticles," *Micro & Nano Letters,* 2017.

[86] Z. Yu, X. Cao, S. Wang, H. Cui, C. Li and G. Zhu, "Research Progress on the Water Stability of a Metal-Organic Framework in Advanced Oxidation Processes," *Water, Air, & Soil Pollution,* vol. 232, no. 1, p. 18, 1 2021.

[87] Q. Li and T. Thonhauser, "A theoretical study of the hydrogen-storage potential of $(H_2)_4CH_4$ in metal organic framework materials and carbon nanotubes," *Journal of Physics Condensed Matter,* vol. 24, no. 42, 2012.

[88] S. Wiggin, "Cambridge Crystallographic Data Centre," 02 09 2020. [Online]. Available: https://www.ccdc.cam.ac.uk/Community/blog/MOF-classification-search-screen/.

List of Figures

Figure 1.1: MOF applications[86] 2
Figure 1.2: MOF publications per year[88] 3
Figure 1.3: MOF for hydrogen storage in fuel cells[28] 5
Figure 1.4: Co_2(*m*-dobdc) pore[28] 6
Figure 1.5: H_2 adsorption isotherm of Co_2(*m*-dobdc) and Ni_2(*m*-dobdc) MOFs [28] ... 6
Figure 1.6: MOF water harvesting devices using MOFs [33] 8
Figure 1.7: Water production in a year for several locations [32] 8
Figure 1.8: MOFs applied to chromatographic columns[37] 10
Figure 1.9: TAMOF-1 crystal structure[38] 11
Figure 1.10: Liquid Chromatography of (±)-ibuprofen[38] 11
Figure 1.11: Polycatenanes degrees of mobility[82] 12
Figure 1.12: Polycatenanes classes[45] 12
Figure 1.13: Example of template-directed approach[48] 13
Figure 1.14: Kinetic and thermodynamic control in the catenane synthesis[49] 14
Figure 1.15: Fast Crystallization Synthesis[68] 16
Figure 1.16: Ball Milling process[85] 18
Figure 1.17: Hard, soft, and intermediate acids in the periodic table[86] 20
Figure 2.1: Mechanochemical synthesis of a1 phase [73] 21
Figure 2.2: PXRD patterns of a) commercial TPB, b) a1 phase with unreacted TPB, c) a1 phase 22
Figure 2.3: PXRD pattern of c1 phase 23
Figure 2.4: TG analysis of crystalline phase[73] 23
Figure 2.5: PXRD patterns of a) a1 phase from NG, b) c1 phase 24
Figure 2.6: IR spectra of a) commercial TPB, b) 1,2-dichlorobenzene 25

Figure 2.7: IR spectra of a) a1 phase, b) c1 phase 26

Figure 2.8: a) CP/MAS ^{13}C solid state NMR spectra of the ligand TPB, b) CP/MAS ^{13}C solid state NMR with non-quaternary suppression [73] 27

Figure 2.9: CP/MAS ^{13}C solid state NMR spectra of a) a1 phase, b) TPB [73] 27

Figure 2.10: HPDec/MAS ^{13}C solid state NMR spectra of a) a1 phase, b) c1 phase [73] 27

Figure 2.11: PXRD pattern of a) commercial TPB, b) TPB recycled from poly-[*n*]-catenane 28

Figure 2.12: PXRD pattern of instant synthesis experiments using a) $ZnBr_2$, b) $ZnCl_2$, c) ZnI_2 30

Figure 2.13: Thermal analysis experiment, PXRD pattern of a) bromide experiment at 240°C, b) chloride experiment at 200°C, c) iodide experiment at 270°C 32

Figure 2.14: PXRD patterns of instant synthesis experiments using a) p-chlorotoluene, b) toluene, c) chloroform 34

Figure 2.15: PXRD patterns of instant synthesis experiments using a) 1,3-dichlorobenzene, b) 1,4-dichlorobenzene 36

Figure 2.16: PXRD pattern of adsorption test using a) 1,2-dCB+1,3-dCB mix, b) 1,2-dCB+1,4-dCB mix 37

Figure 2.17: PXRD pattern of instant synthesis experiment using 1,4-dichlorobenzene 38

Figure 2.18: Suzuki-Miyaura Coupling cycle[84] 39

Figure 2.19: Synthesis of 1,3,5-tri(pyridin-4-yl)benzene (**2**) 40

Figure 2.20: a) 1H NMR spectrum of commercial TPB; 40

Figure 2.21: First assumed route for the synthesis of compound (**5**) 41

Figure 2.22: Second route for the synthesis of compound (**5**) 41

Figure 2.23: ^1H NMR spectrum of compound (**3**) 42

Figure 2.24: ^1H NMR spectrum of compound (**4**) 43

Figure 2.25: ^1H NMR spectrum of compound (**5**) 43

Figure 2.26: Synthesis of 1,3,5-tri(pyridin-4-yl)benzene (**6**) 44

Figure 3.1: ^{1}H NMR spectrum of compound (**1**) 49
Figure 3.2: ^{1}H NMR spectrum of compound (**2**) 50
Figure 3.3: ^{1}H NMR spectrum of compound (**3**) 51
Figure 3.4: ^{1}H NMR spectrum of compound (**4**) 52
Figure 3.5: ^{1}H NMR spectrum of compound (**5**) 53

Ringraziamenti

In primo luogo, vorrei ringraziare il mio relatore, il Professor Javier Martí-Rujas, che mi ha seguito nel mio percorso di tesi. In questo anno di lavoro, con il Suo ricco sapere e la Sua disponibilità, mi ha guidato e coinvolto nella ricerca sperimentale, insegnandomi tutto il necessario per farmi appassionare a questa attività.

Un sentito ringraziamento va al Professor Alessandro Sacchetti, senza il quale non avrei intrapreso questo percorso. Con la Sua profonda conoscenza nell'ambito chimico mi ha aiutato a districarmi tra le difficoltà della sintesi organica.

Ringrazio il mio controrelatore, il Dottor Manfredi Caruso. Senza di lui non sarei riuscito a sopravvivere alle attività di laboratorio e alla stesura di questo elaborato. In questo periodo mi ha sempre affiancato e ispirato, trasmettendomi le conoscenze che lui stesso ha appreso negli scorsi anni di dottorato.

La mia gratitudine va anche a tutti i professori del gruppo OSCMLab, sempre disponibili e pronti nei consigli.

Ringrazio tutti i dottorandi che ho conosciuto in dipartimento. Ognuno mi ha insegnato qualcosa, siete stati in grado di aiutarmi, non solo nel lavoro svolto, ma anche dimostrando supporto ogni giorno. Questo ha permesso di fondare sinceri rapporti di amicizia con ciascuno di voi.

A tutti i colleghi. La vostra presenza è stata indispensabile per il mio percorso universitario. Ai compagni di università con i quali ho condiviso le gioie di questi cinque anni, per il vicendevole supporto negli esami e per i momenti memorabili fuori dall'ambito accademico. Ai compagni di laboratorio con cui ho condiviso il percorso di tesi nell'ultimo anno; l'unione di vecchie e nuove amicizie ha permesso di creare un ambiente perfetto sia per superare la fatica e le difficoltà del lavoro, sia per il divertimento garantito nelle occasioni di pausa e nei ritrovi al di fuori del dipartimento.

Un ringraziamento speciale è diretto ad Andrea Magri. Compagno di avventure di questi anni si è dimostrato essere un amico fedele su cui contare. La sua presenza ha reso divertenti e indimenticabili le giornate passate in università e in laboratorio.

Infine, il ringraziamento più importante va ai miei genitori. Mi hanno sempre sostenuto e consigliato, ciascuno a modo proprio, per superare i problemi e ottenere il meglio da me stesso. Senza di loro, più di ogni altro, non sarei stato in grado di raggiungere questo traguardo che dedico a loro.